

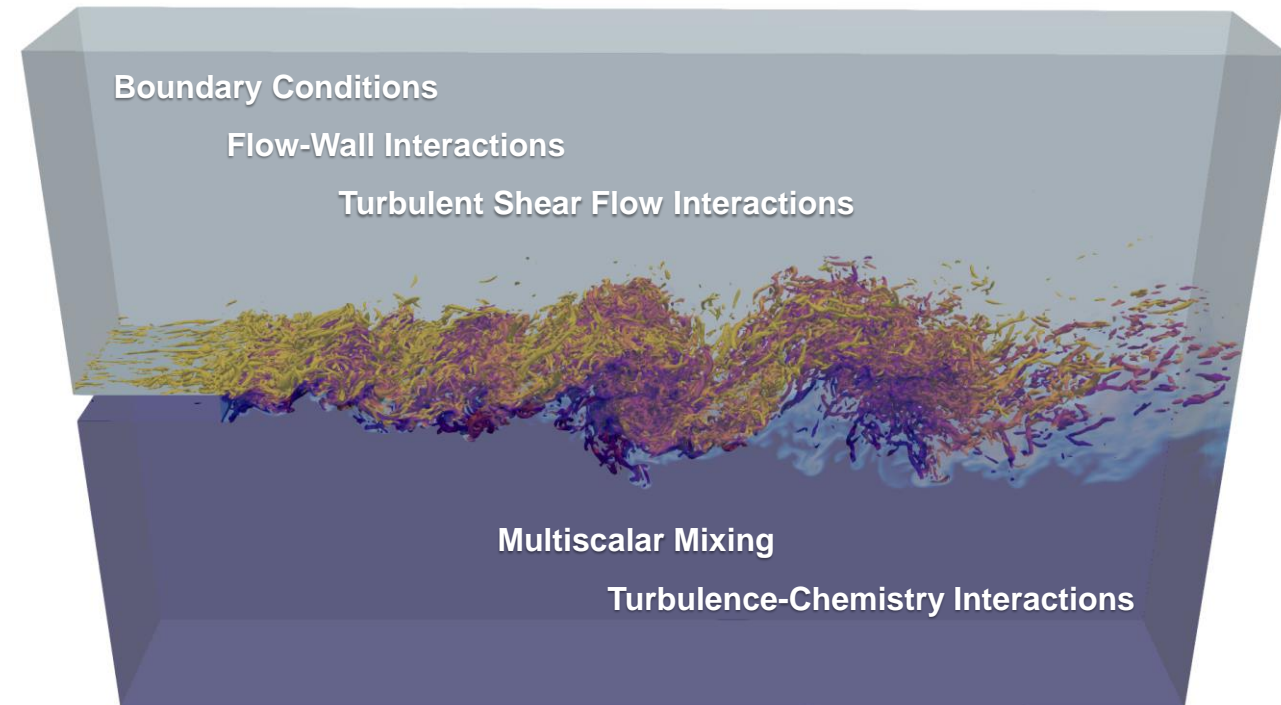
Advanced Model Development for Large Eddy Simulation of Oxy-Combustion and Supercritical CO₂ Power Cycles

Dhruv Purushotham, Chang Hyeon Lim
Joe Oefelein, Adam Steinberg, Devesh Ranjan

Daniel Guggenheim School of Aerospace Engineering
George W. Woodruff School of Mechanical Engineering
Georgia Institute of Technology, Atlanta GA

Overarching objective is accurate implementation of LES so it can be applied with refined precision and control

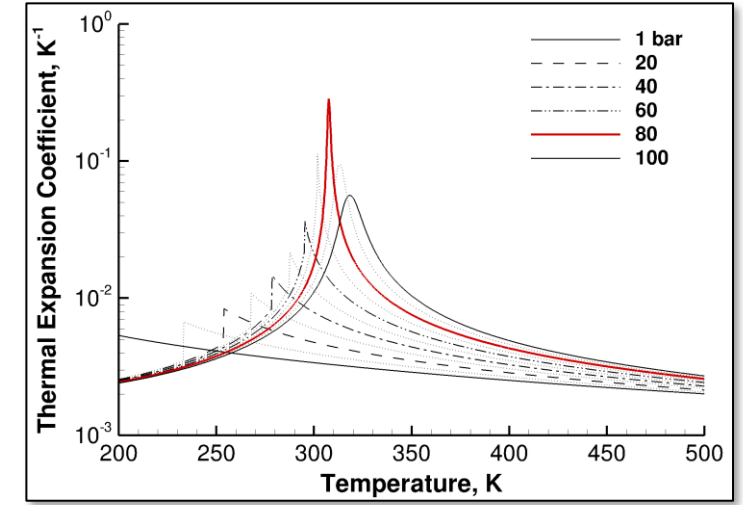
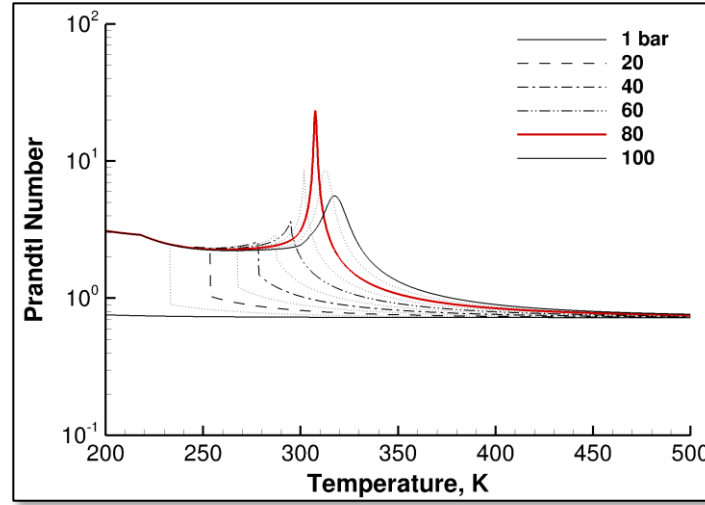
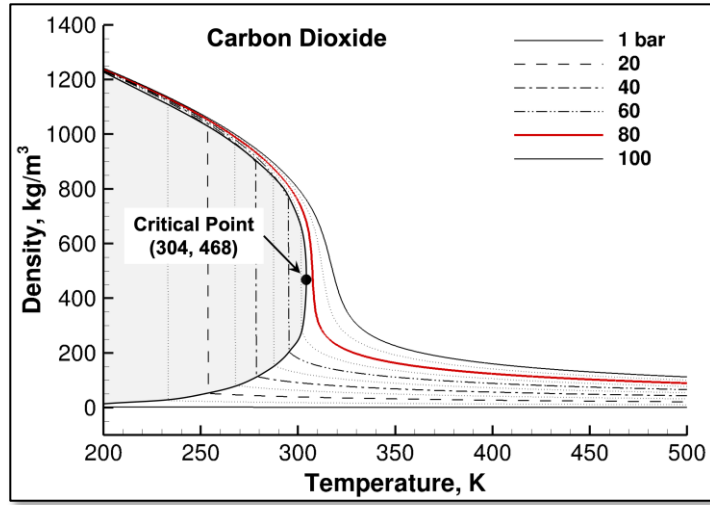
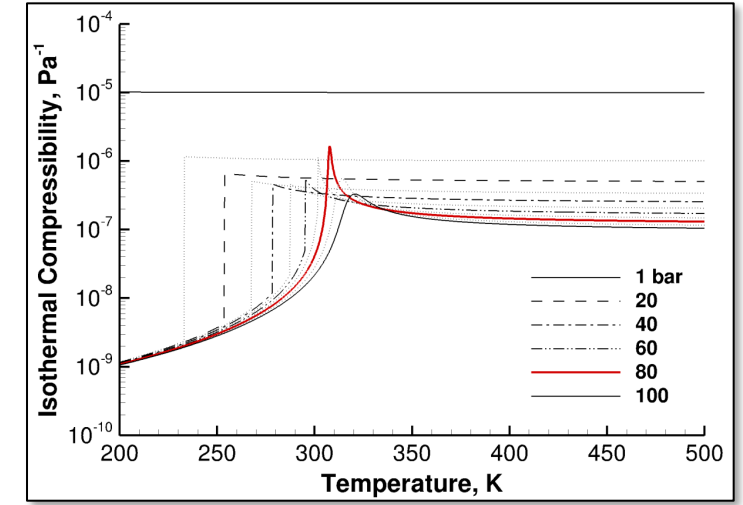
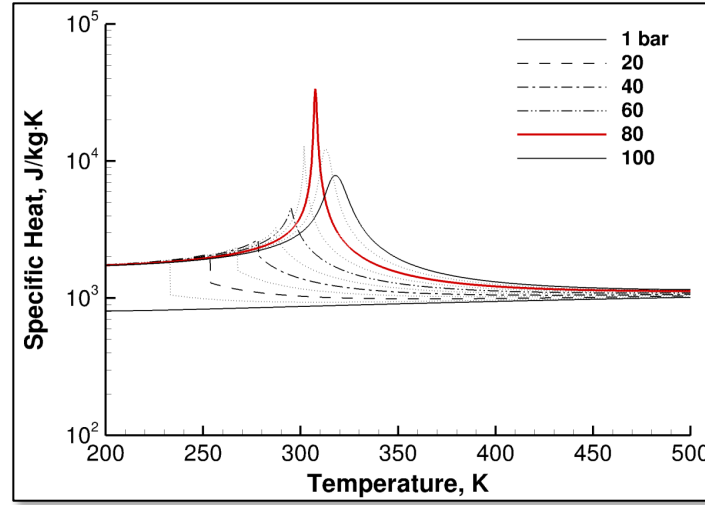
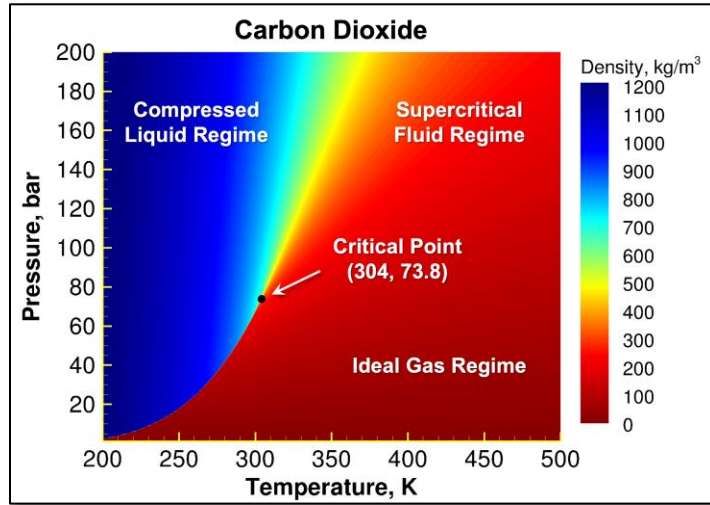
- Physics of interest involves strongly coupled multiscale/multiphysics phenomena
 - High-Reynolds-number turbulence and multiscalar mixing processes ($Re \gg 100,000$)
 - High-pressure multi-regime combustion
 - Compressible, acoustically active flow
 - Complex fuels, multiphase flow
 - Complex geometries
- Many processes poorly understood, no one research approach gives complete information
 - Simulations only treat limited ranges of scales
 - Experiments provide limited information
 - Many sources of uncertainty
- True validation is difficult, tradeoffs between cost and accuracy are always prohibitive



Compounding factors

- Many assumptions applied for multiphysics problems have not been formally justified; e.g., LES of compressible reacting flows
 - LES initially developed for inert incompressible flows, extension to multiphysics systems has evolved by analogy not rigorous evaluation of basic assumptions
 - Additional terms that arise as a consequence of filtering the compressible multicomponent conservation equations are typically neglected
 - Significant nonlinearities are introduced due to compressibility effects and nonideal behavior associated with thermodynamic and transport properties, etc.
- No formal guidelines that quantify the required spatial or temporal resolution for accurate implementation of LES due to model complexity and nonlinearities, etc.
 - Different systems of subfilter models will have different requirements regarding ranges of scales they can accurately represent
 - Existing models are not always implemented “consistently” with rigorous resolution requirements in mind (i.e., resolution based on what is computationally affordable)
 - New models may be required to account for additional terms such as scalar-scalar covariances

Supercritical fluids pose unique additional modeling challenges due to highly nonlinear property variations

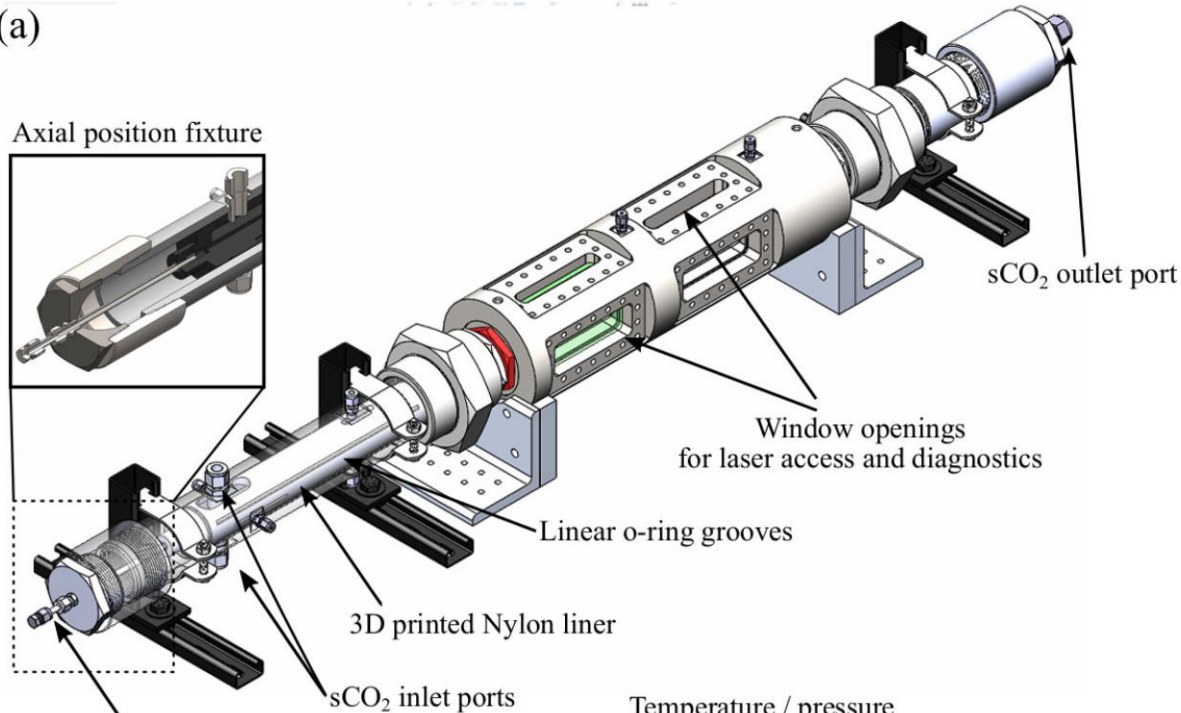


Tasks/milestones completed and current focal points

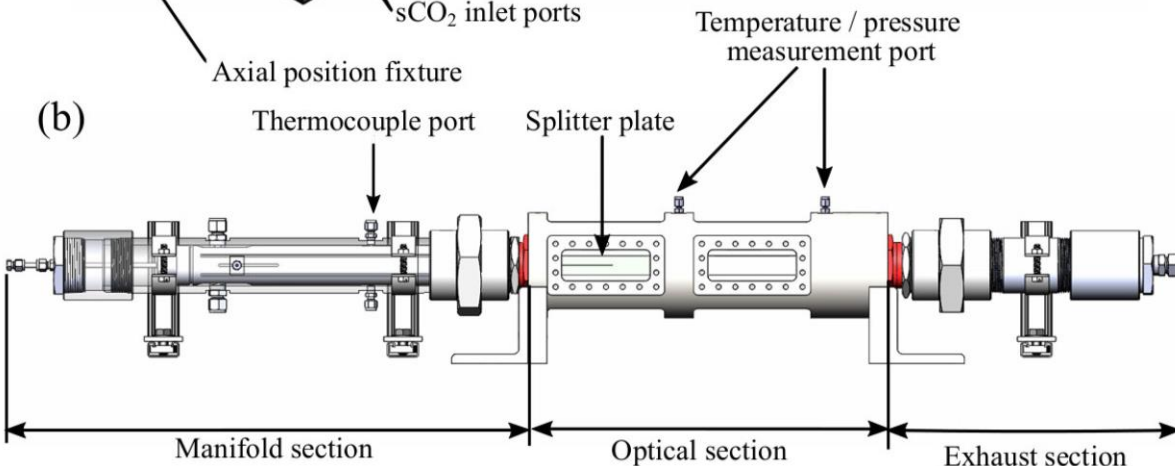
- **Task 1.0: Project Management and Planning**
- **Task 2.0: Multiphysics Model Development**
 - Subtask 2.1: Unit physics model evaluation and verification studies
 - Subtask 2.2: Treatment of turbulent multiscale mixing processes
 - Subtask 2.3: Treatment of turbulence-chemistry interactions
- **Task 3.0: Benchmark Large Eddy Simulations**
 - Subtask 3.1: Model validation (Georgia Tech sCO₂ Loop)
 - Subtask 3.2: Model validation (SwRI 1 MW Oxy-Fueled sCO₂ Combustor)
 - Subtask 3.3: Parametric Analysis
- **Task 4.0: Experiments for Model Validation**
 - Subtask 4.1: Non-reacting density and velocity measurements in redesigned test section
 - Subtask 4.2: Preliminary IR measurements in 1 MW oxy-fueled sCO₂ combustor
 - Subtask 4.3: Complete IR measurements in 1 MW oxy-fueled sCO₂ combustor

Georgia Tech sCO₂ loop designed to provide insights into supercritical fluid mixing (80 bar , $308 \leq T \leq 318 \text{ K}$)

(a)



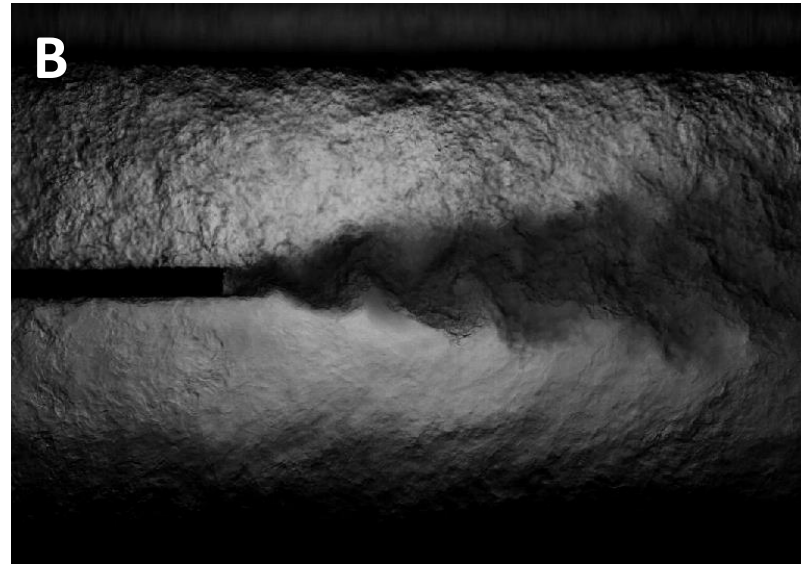
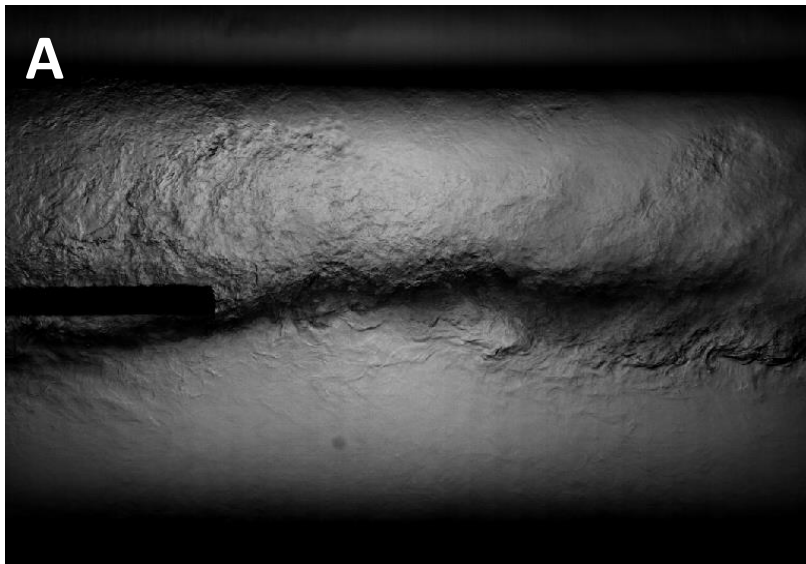
(b)



	Pressure [MPa / psi]	Temperature [K / F]	Re	Density [kg/m ³]	Velocity [m/s]
Upper Stream	8 / 1160	308 / 94.7	1.26e5	419.08	0.55
Lower Stream	8 / 1160	318 / 113	4.48e4	241.04	0.11

Experimental techniques: high-speed shadowgraphy, high-speed schlieren, spontaneous Raman scattering

Date	Run #	Pressure (MPa)	Temperature (K)		Mass Flow (kg/s)		Mass Flow Ratio	Density (kg/m ³)		Density Ratio	Velocity (m/s)		Atwood Number	Note
	A	8	318	308	0.0415	0.015	2.77	241	417.67	1.73	0.53	0.11	0.27	Baseline
	B	8	308	318	0.05	0.03	1.67	417.67	241	0.58	0.37	0.39	0.27	RT
	C	8	308	318	0.02	0.04	0.50	417.67	241	0.58	0.15	0.51	0.27	



Representative Shadowgraphs

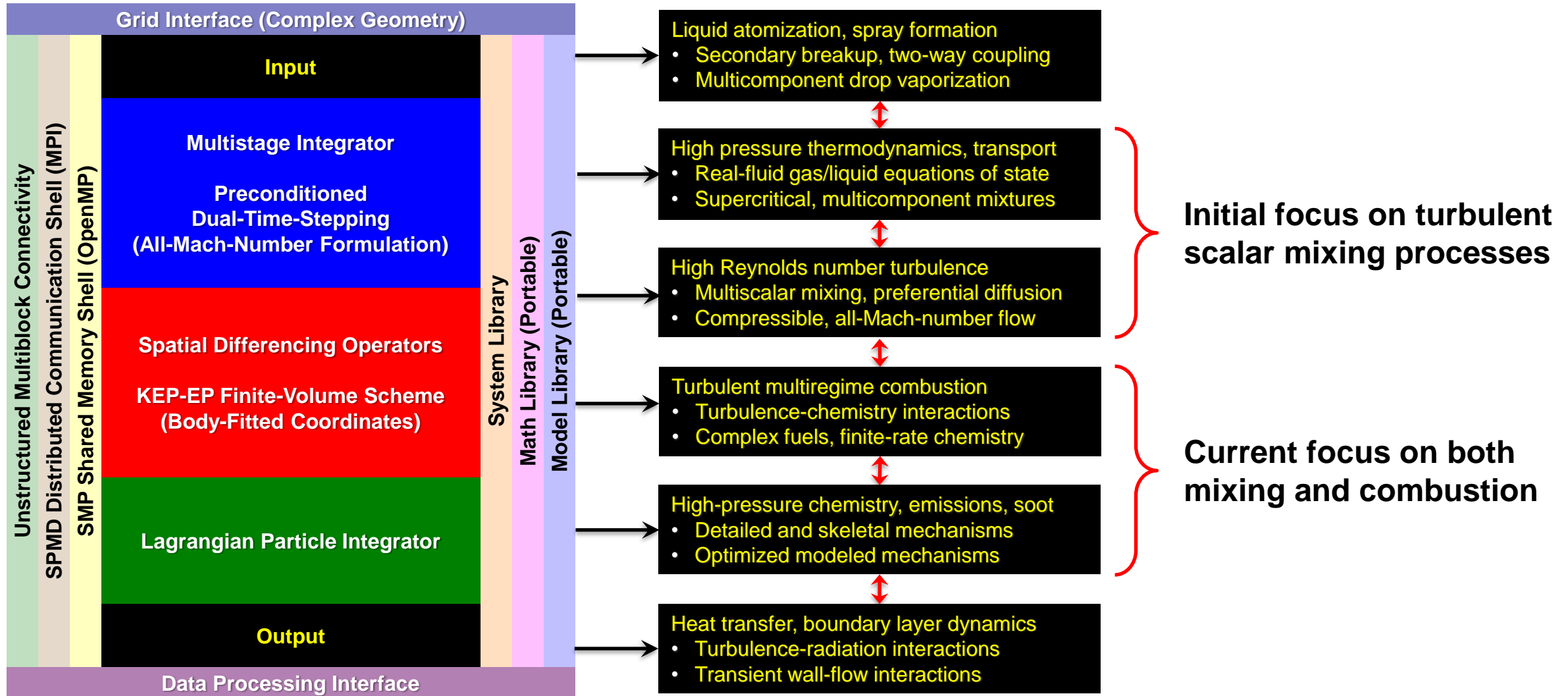
Simulations performed using RAPTOR code framework combined with access to ORNL Summit platform

- Theoretical framework (Comprehensive)
 - Fully-coupled, compressible conservation equations
 - Nonideal gas/liquid equation of state (high-pressure phenomena)
 - Detailed thermodynamics, transport, finite-rate chemistry
 - Multiphase flow (interface tracking via LS-VOF-GFM, drops via L-E formulation)
 - Dynamic subfilter modeling (no tuned constants)
 - Fully integrated CHT and FSI (in progress)
- Numerical framework (High-quality)
 - Kinetic-energy/entropy preserving (non-dissipative, discretely conservative)
 - All-Mach-number (dual-time stepping with generalized preconditioning)
 - Complex geometry and BC's
- Massively-parallel (Highly-scalable)



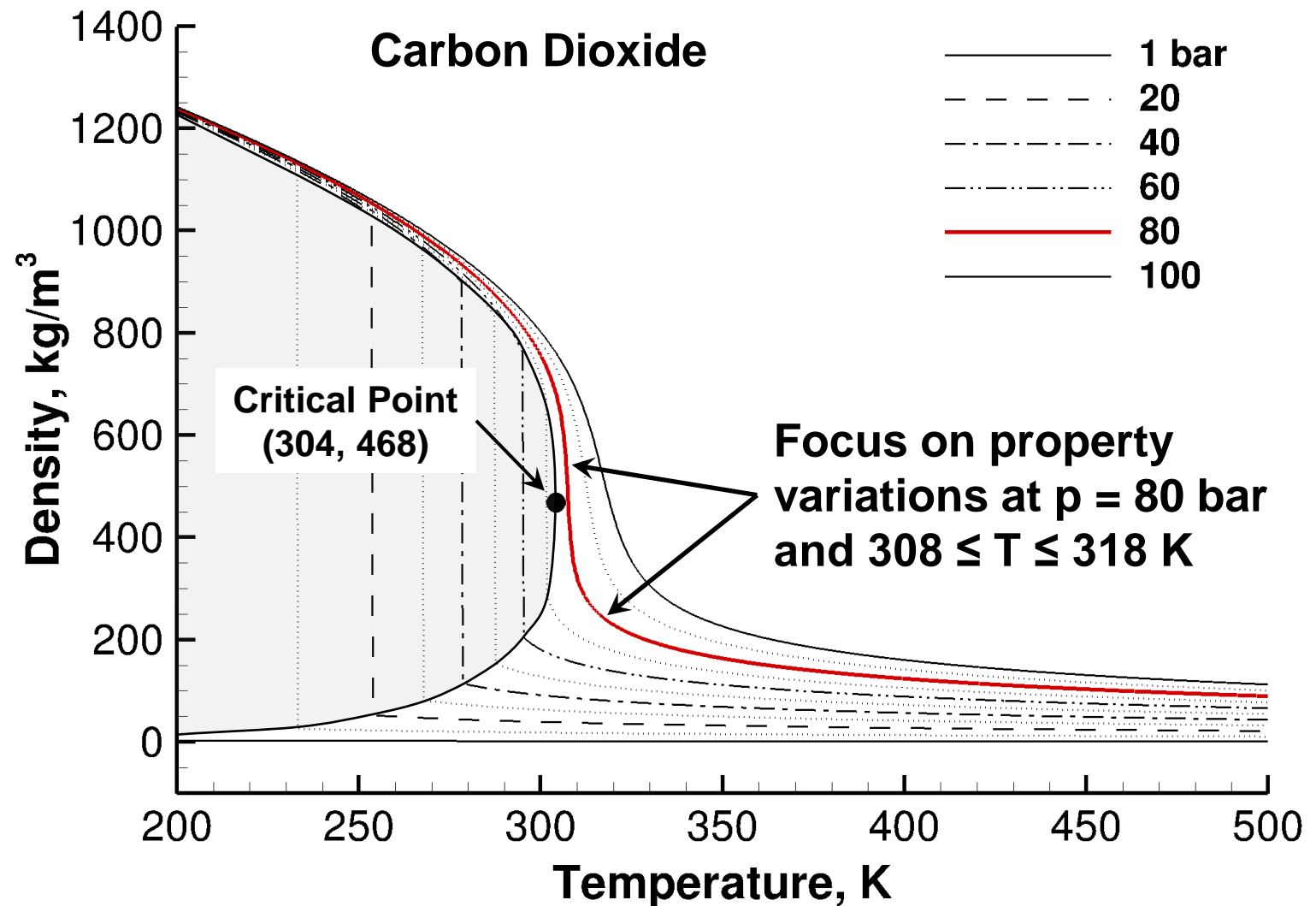
Project selected to receive 2021-2022 ASCR Leadership Computing Challenge (ALCC) award

Simulations performed using RAPTOR code framework combined with access to ORNL Summit platform

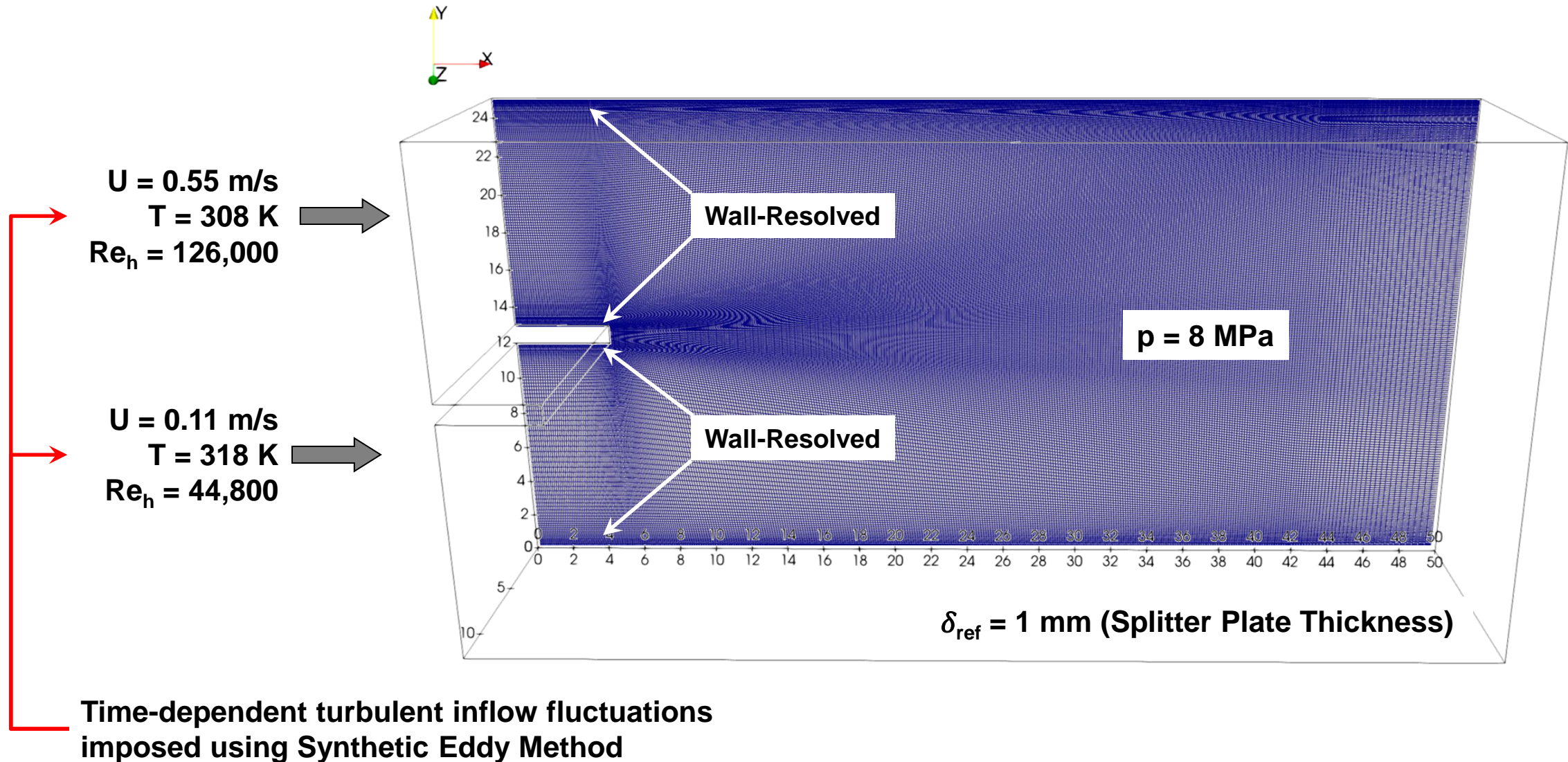


Conditions selected to induce strong nonlinear property variations across mixing layer

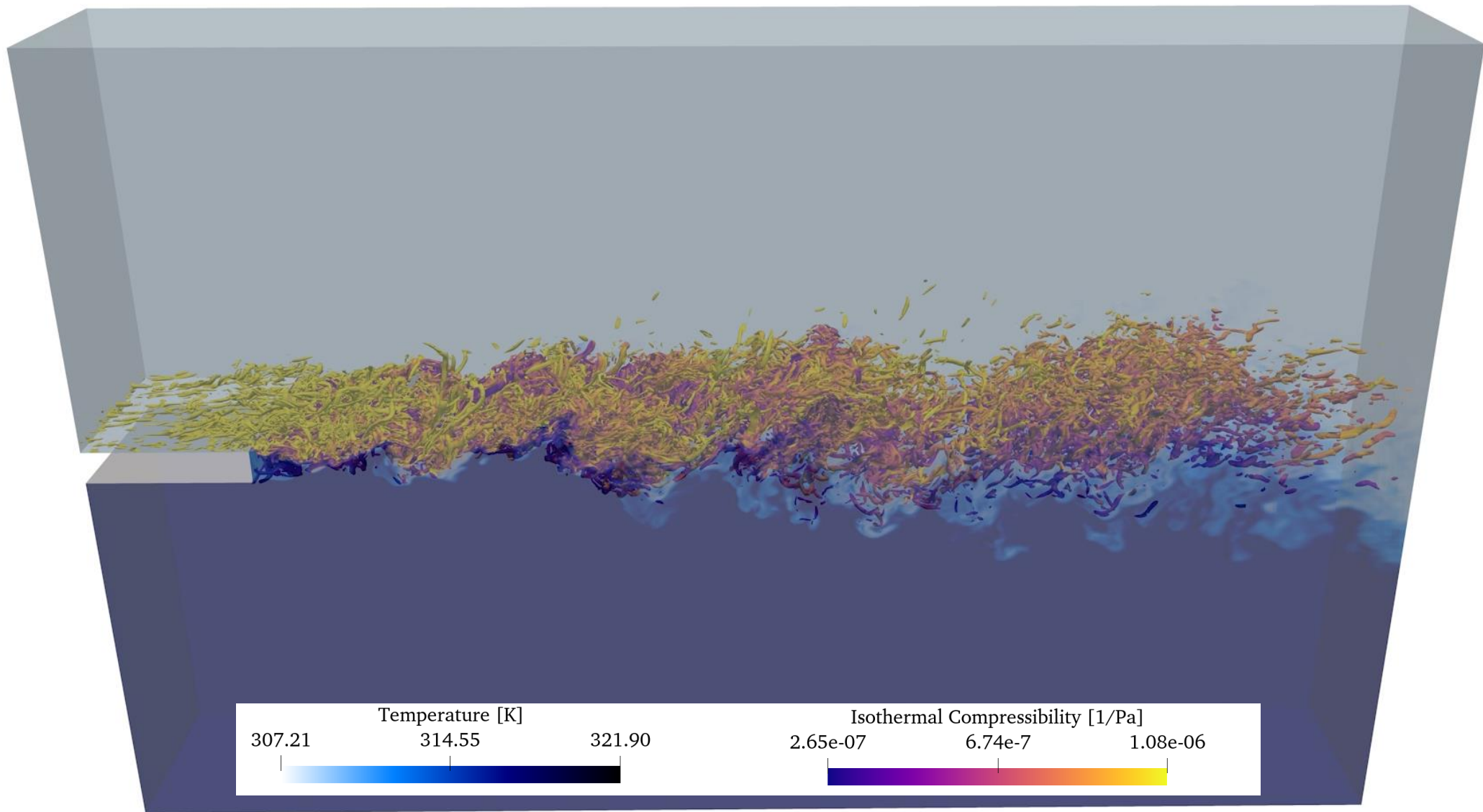
- State-of-the-art formulation for EOS, thermodynamics, transport, and interfacial properties based on NIST expertise over decades
 - Real-fluid mixture properties obtained using Extended Corresponding States model
 - Multicomponent formulation using Cubic (e.g., SRK, PR), BWR, or Helmholtz EOS
 - Generalized to treat wide range of hydrocarbon mixtures (Fuel/Oxidizer/Products)
- Custom stand-alone software designed to run efficiently on HPC platforms



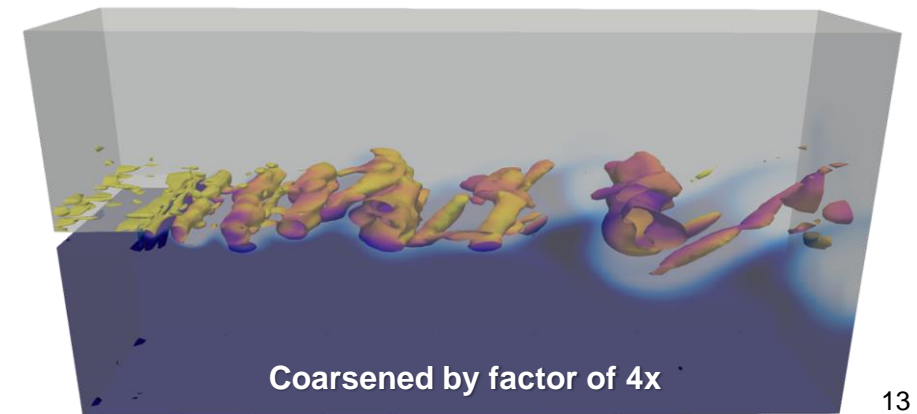
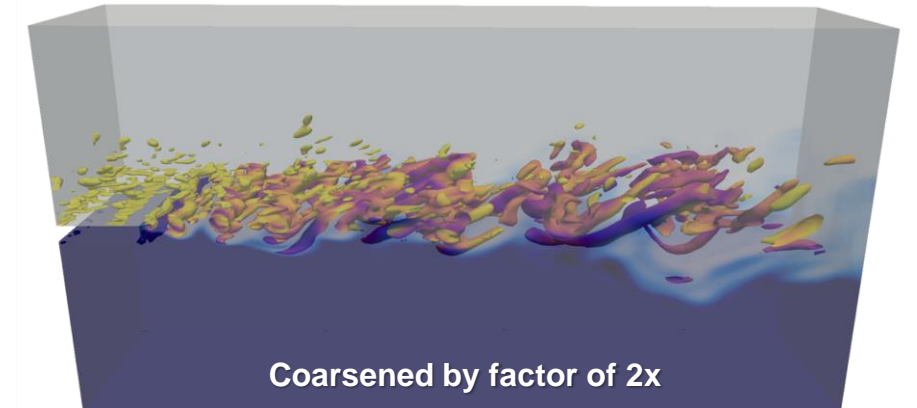
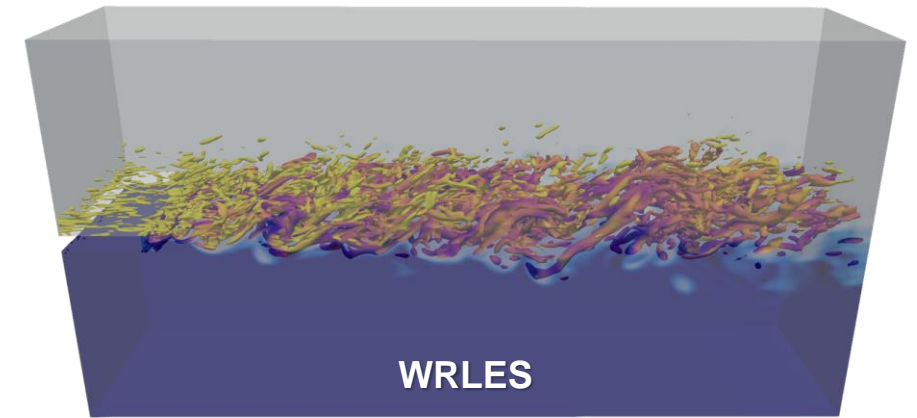
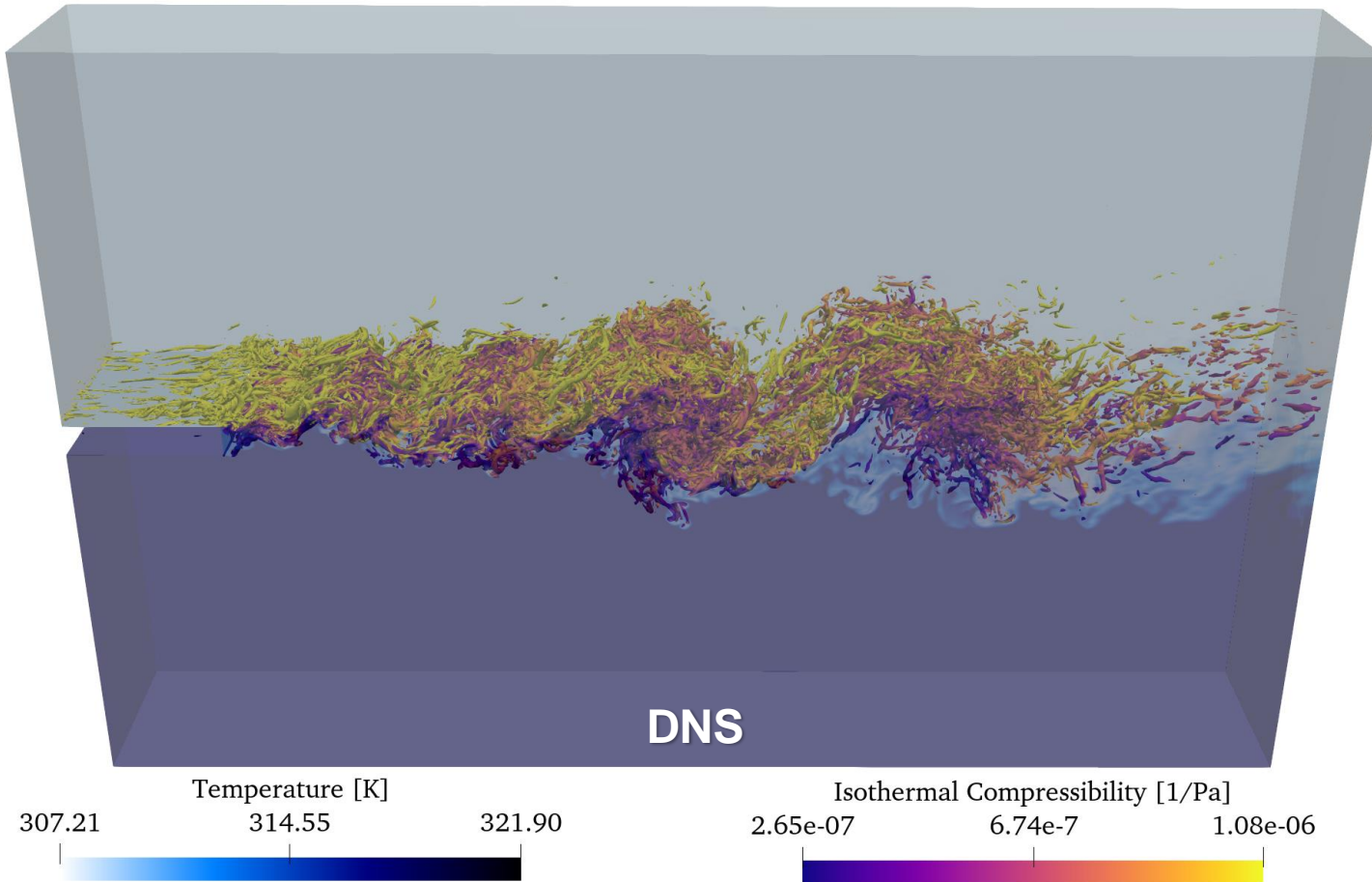
Computational domain and grid match experiment, sequence of 4 cases completed (DNS, WRLES, /2x, /4x)



Baseline DNS

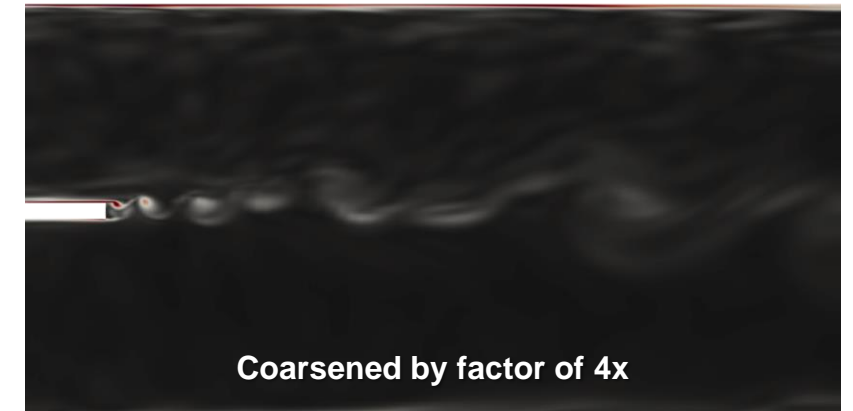
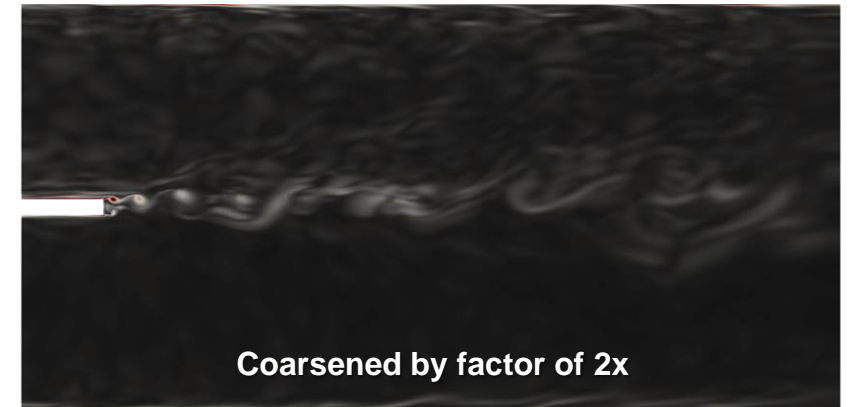
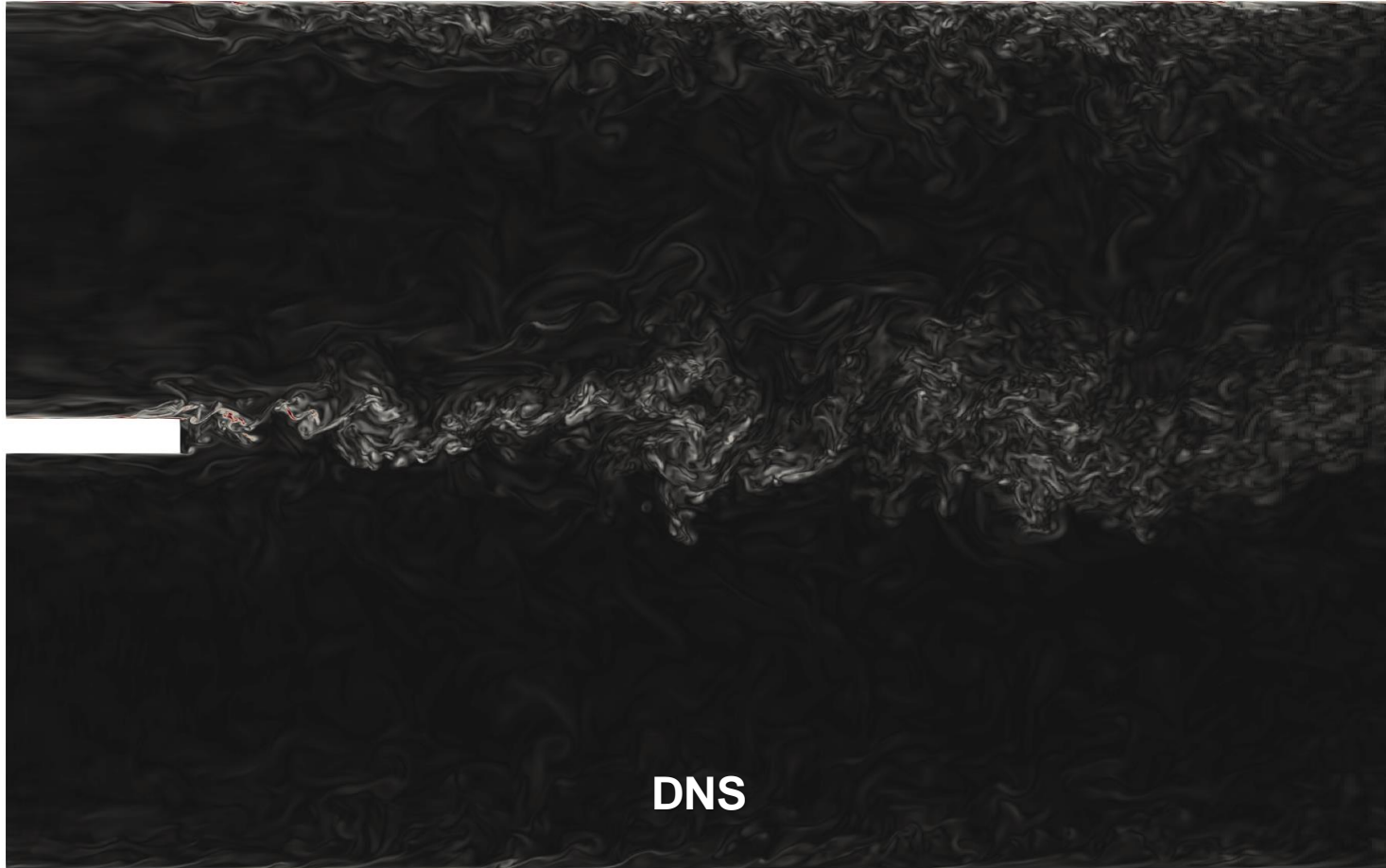


Turbulence structure as function of resolution

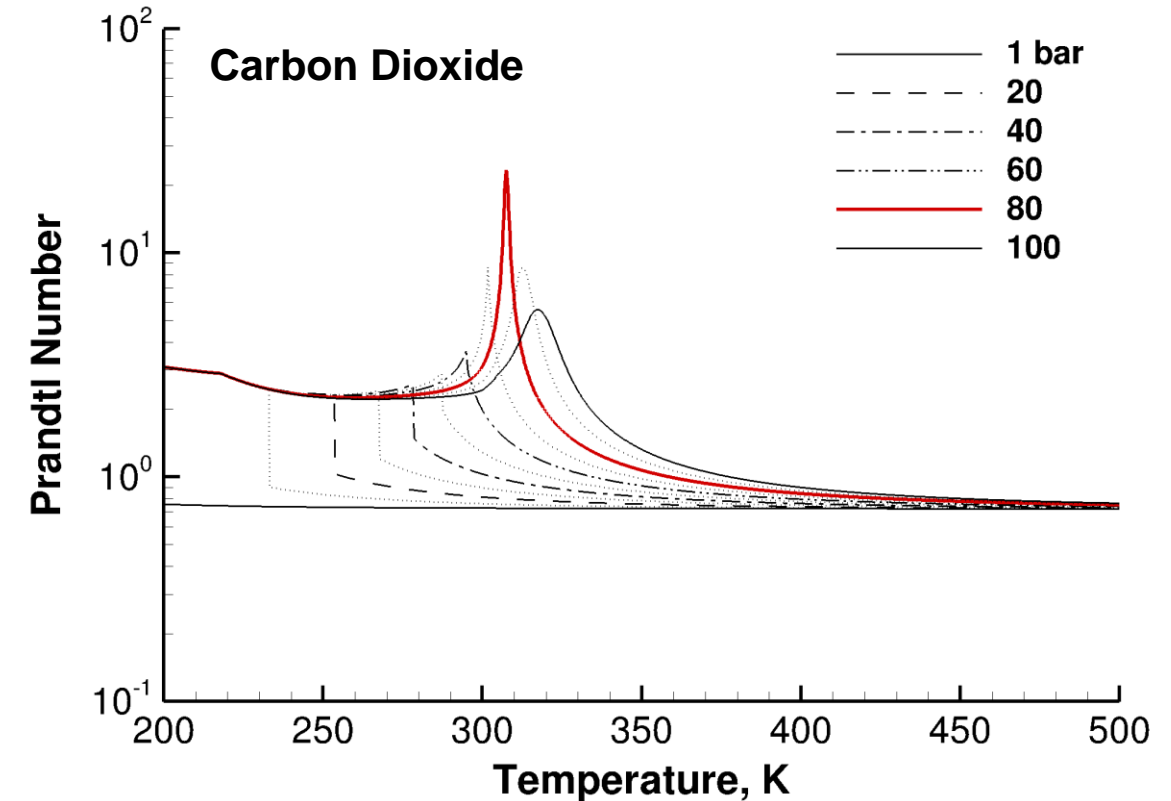
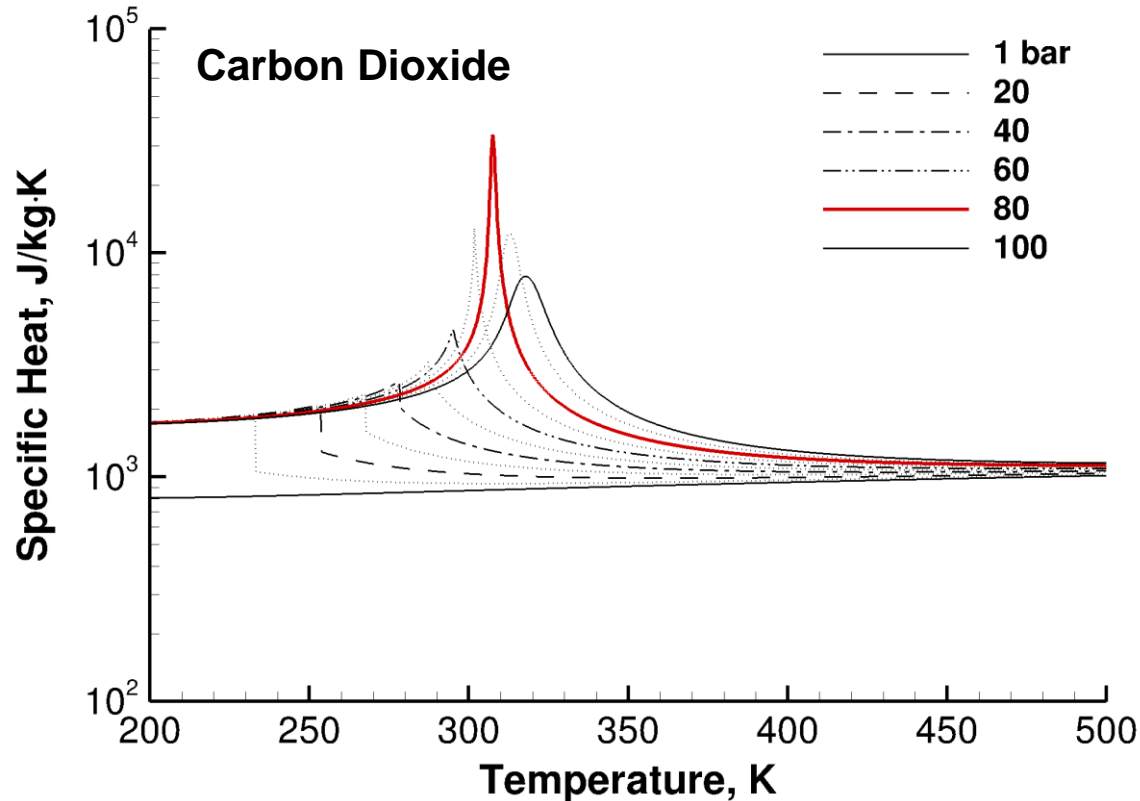


Cross-section of the magnitude of vorticity [1/s]

0.00e+00 1.75e+3 3.50e+03

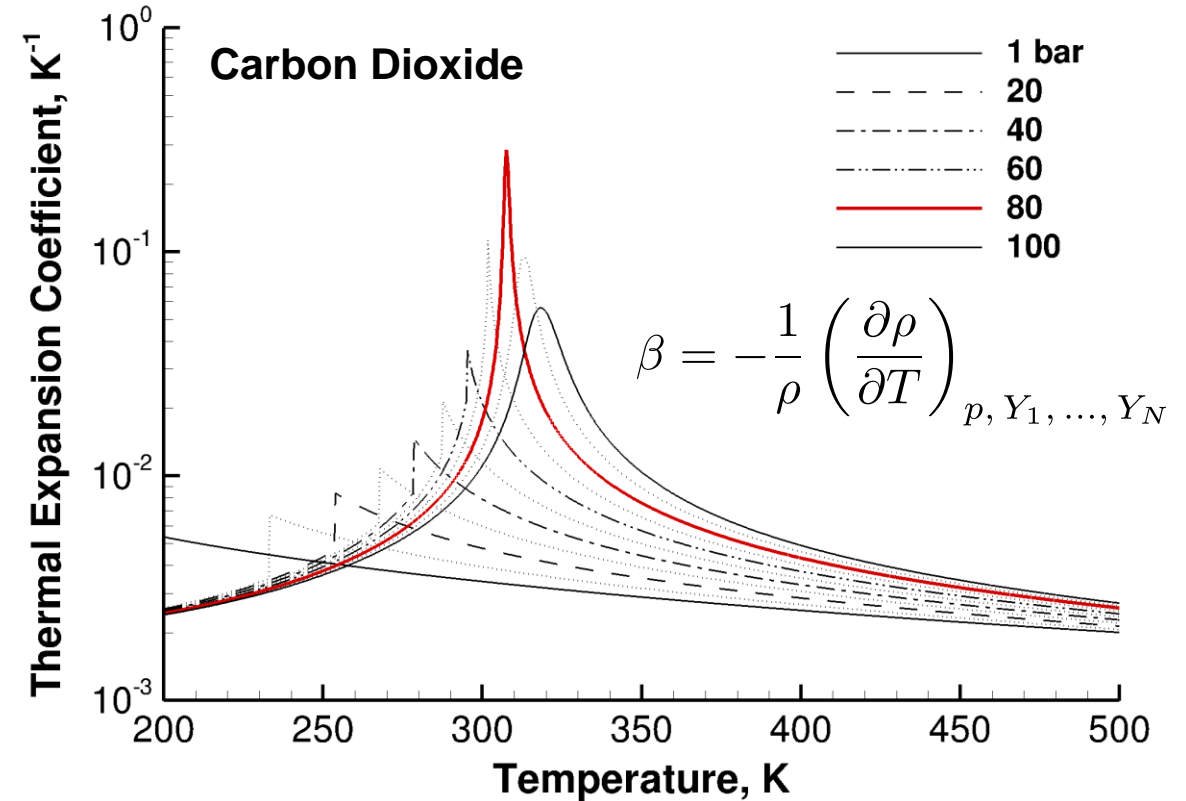
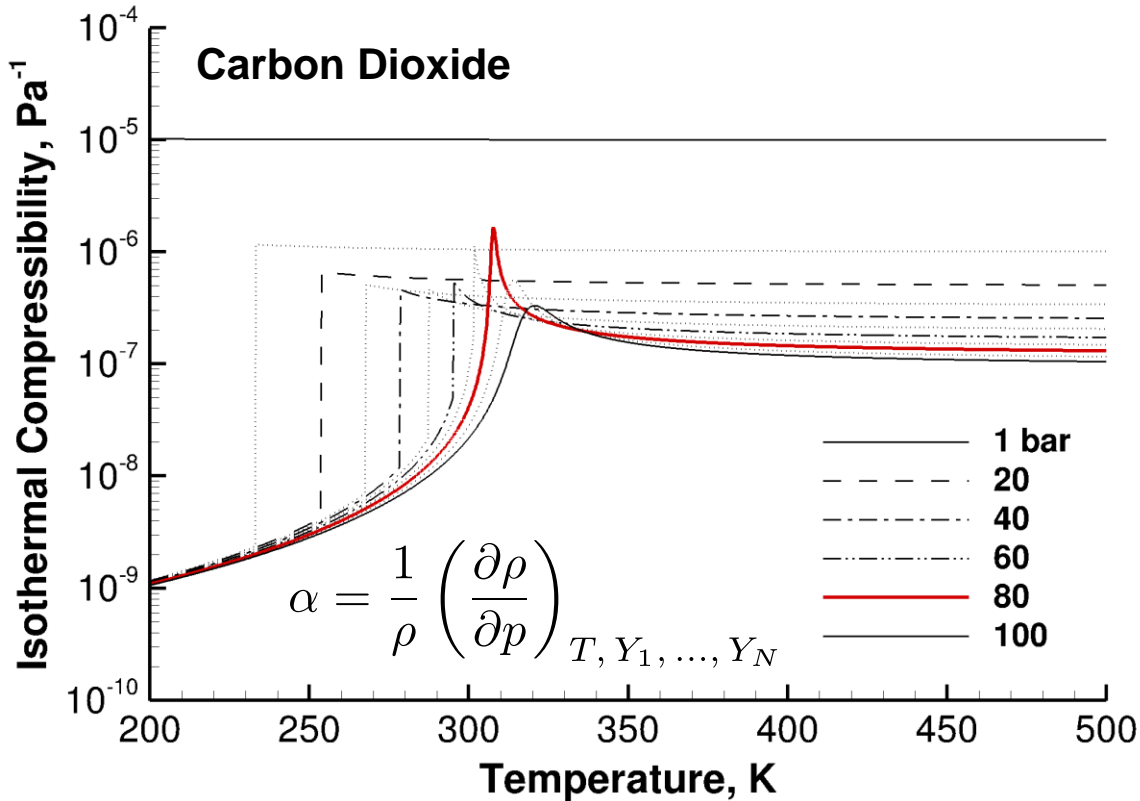


How do nonlinear property variations affect flow and what are the implications with respect to modeling?



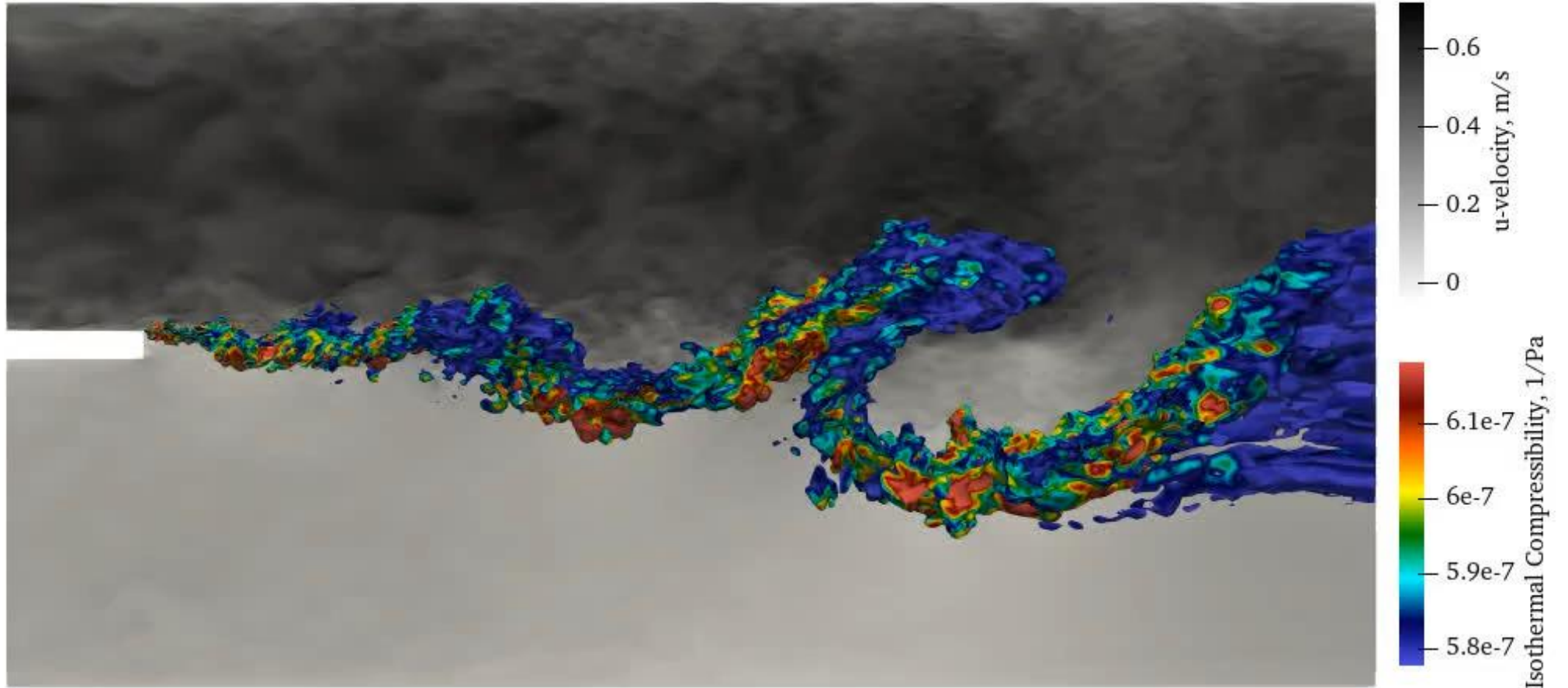
- Heat capacity of the fluid increases dramatically (e.g., more than an order of magnitude between 1 bar and 80 bar over the interval $308 \leq T \leq 318$ K)
- Similarly, significant increases in the Prandtl number are induced (e.g., more than an order of magnitude between 1 bar and 80 bar over the interval $308 \leq T \leq 318$ K)

How do nonlinear property variations affect flow and what are the implications with respect to modeling?



- Two forms of compressibility must be considered
 - Isothermal compressibility ... change in volume due to change in pressure at constant temperature
 - Coefficient of thermal expansion ... change in volume due to change in temperature at constant pressure

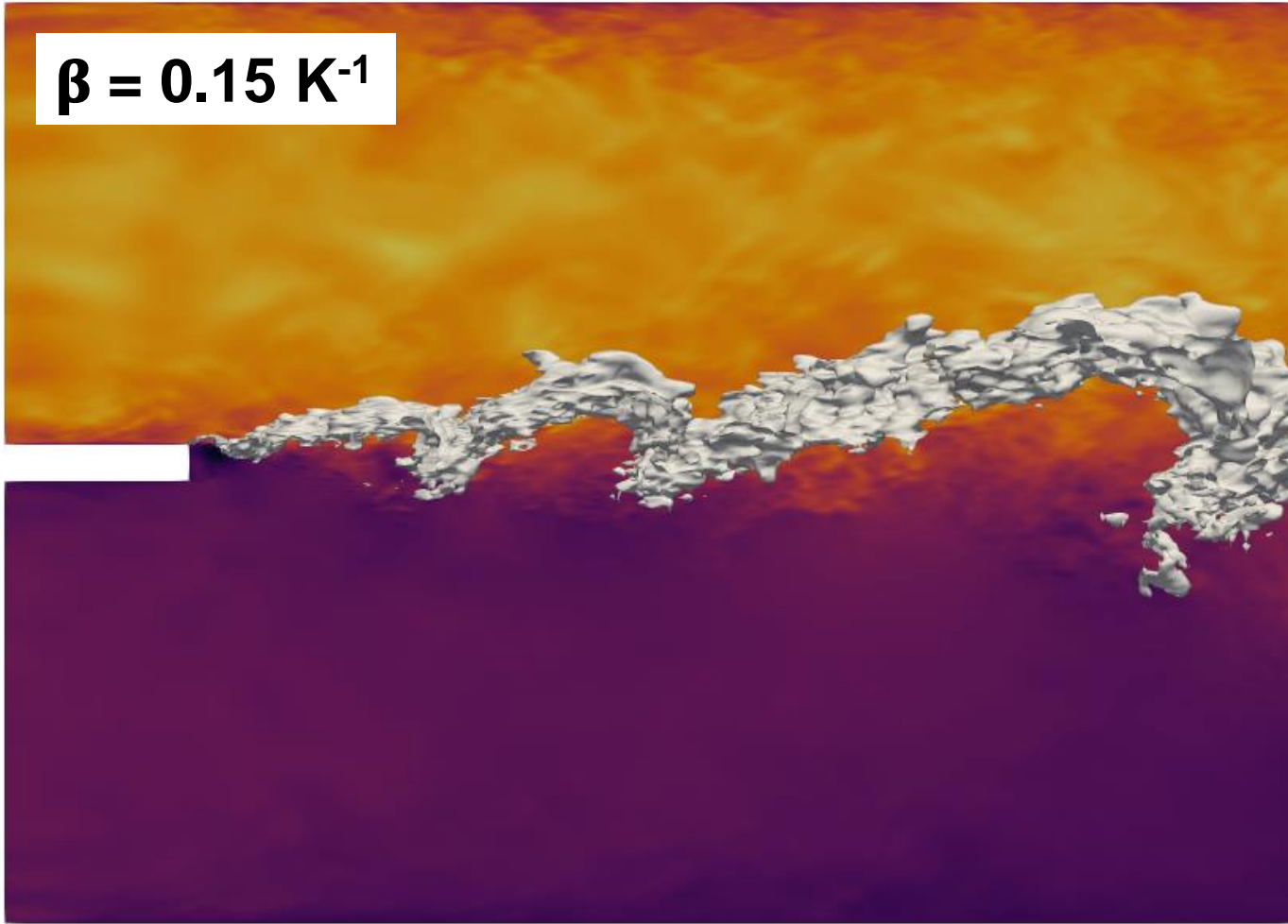
Variation of isothermal compressibility across three-dimensional mixing layer



$$\alpha = \frac{1}{\rho} \left(\frac{\partial \rho}{\partial p} \right)_{T, Y_1, \dots, Y_N}$$

Nonlinearities associated with different quantities affect different regions of the flow

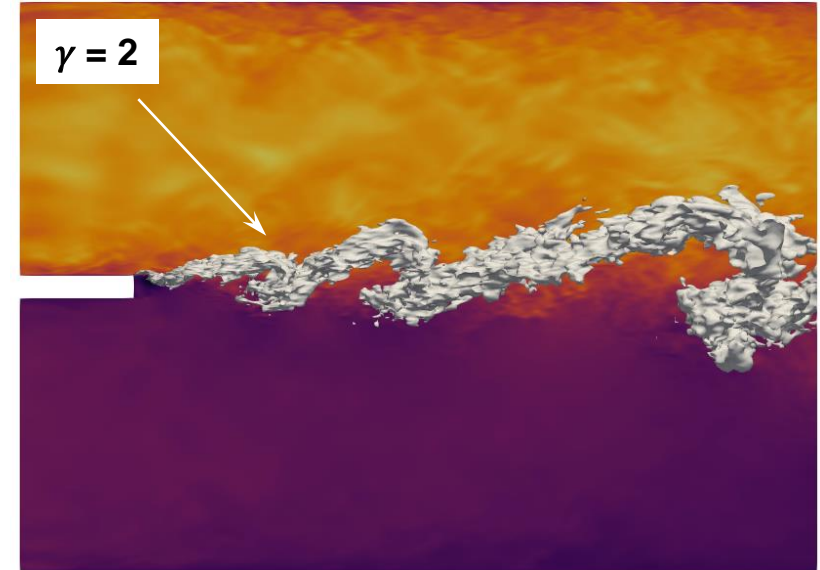
$\beta = 0.15 \text{ K}^{-1}$



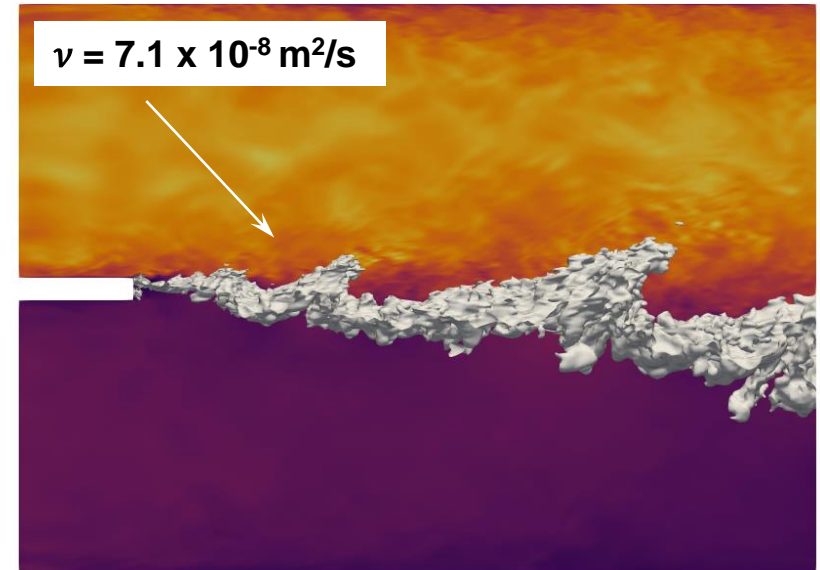
u-velocity, m/s

0.6
0.4
0.2
0
-0.2

$\gamma = 2$



$\nu = 7.1 \times 10^{-8} \text{ m}^2/\text{s}$



$$\beta = -\frac{1}{\rho} \left(\frac{\partial \rho}{\partial T} \right)_{p, Y_1, \dots, Y_N}$$

Rate of change in pressure and temperature can be significantly modulated by these nonlinearities

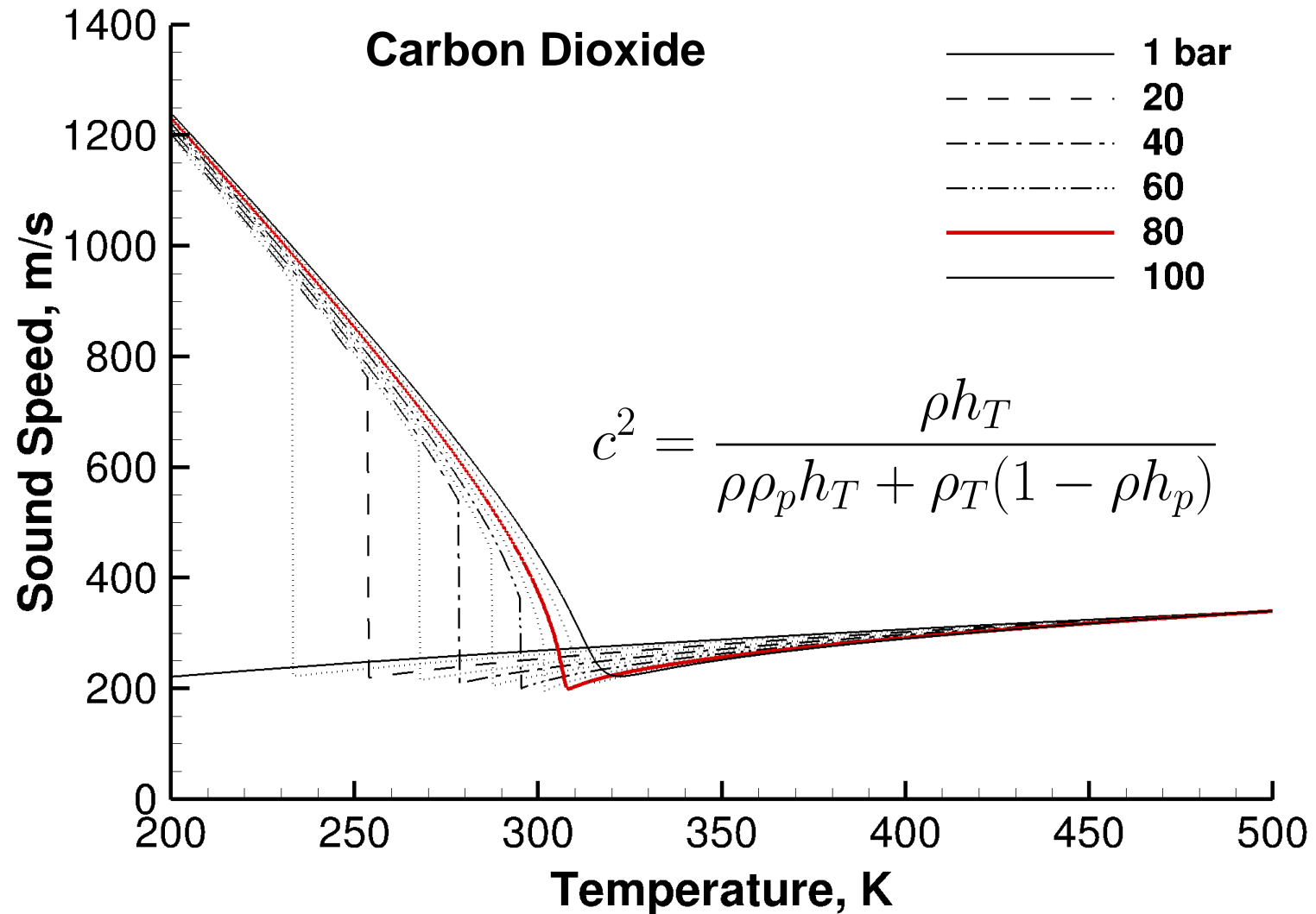
$$\begin{aligned}
 \frac{\partial p}{\partial t} = & -\frac{c^2}{\rho C_p} \left\{ \left[\rho_T h + \rho C_p - \sum_{i=1}^{N-1} (\rho_T h_{Y_i} - \rho_{Y_i} C_p) Y_i \right] \underbrace{\nabla \cdot (\rho \mathbf{u})}_{\text{Mass}} \right. \\
 & + \rho_T \left(\underbrace{\mathbf{u} \cdot \nabla p + M^2 \tau : \nabla \mathbf{u}}_{\text{Momentum}} - \underbrace{\nabla \cdot (\rho h \mathbf{u}) + \nabla \cdot \mathbf{q}_e}_{\text{Total Energy}} \right) \\
 & \left. + \sum_{i=1}^{N-1} (\rho_T h_{Y_i} - \rho_{Y_i} C_p) \left(\underbrace{\nabla \cdot (\rho Y_i \mathbf{u}) - \nabla \cdot \mathbf{q}_i - \dot{\omega}_i}_{\text{Species}} \right) \right\} \\
 \frac{\partial T}{\partial t} = & \frac{c^2}{\rho C_p} \left\{ \left[\rho_p h + \rho_T \frac{T}{\rho} - \sum_{i=1}^{N-1} \left(\rho_p h_{Y_i} - \rho_{Y_i} \rho_T \frac{T}{\rho^2} \right) Y_i \right] \underbrace{\nabla \cdot (\rho \mathbf{u})}_{\text{Mass}} \right. \\
 & + \rho_p \left(\underbrace{\mathbf{u} \cdot \nabla p + M^2 \tau : \nabla \mathbf{u}}_{\text{Momentum}} - \underbrace{\nabla \cdot (\rho h \mathbf{u}) + \nabla \cdot \mathbf{q}_e}_{\text{Total Energy}} \right) \\
 & \left. + \sum_{i=1}^{N-1} \left(\rho_p h_{Y_i} - \rho_{Y_i} \rho_T \frac{T}{\rho^2} \right) \left(\underbrace{\nabla \cdot (\rho Y_i \mathbf{u}) - \nabla \cdot \mathbf{q}_i - \dot{\omega}_i}_{\text{Species}} \right) \right\}
 \end{aligned}$$

where

$$\frac{c^2}{\rho C_p} = \frac{1}{\rho_p \rho C_p + \rho_T (1 - \rho h_p)} = \frac{1}{\rho} \left[\frac{1}{\alpha \rho C_p - \beta (1 - \rho h_p)} \right] = \frac{1}{\rho} \left[\frac{1}{\alpha \rho C_p - \beta^2 T} \right]$$

Impact of thermodynamic and transport anomalies at supercritical conditions

- Thermodynamic nonidealities and transport anomalies impose additional nonlinearities that modulate both broadband turbulence characteristics and observables (e.g., multiscale mixing)
- Alters both the instantaneous and filtered equations for LES identically*
 - i.e., they premultiply convective/diffusive operators and source terms in both sets of equations and thus modulate these terms in the same way
 - *Additional focus needs to be placed on filtering nonlinear EOS, internal energy, enthalpy, etc.
- Chemical source term Jacobians and related eigenvalues also involve ρ_p and ρ_T
 - i.e., compressibility and thermodynamic nonidealities also affect finite-rate chemical kinetics and related stiffness in chemistry
- Nonequilibrium turbulence, baroclinic torque, etc., also significant factors



Many additional terms arise as consequence of filtering compressible multicomponent conservation equations

- Filtered Mass:

$$\frac{\partial \bar{\rho}}{\partial t} + \nabla \cdot (\bar{\rho} \tilde{\mathbf{u}}) = 0. \quad (1)$$

- Filtered Momentum:

$$\frac{\partial}{\partial t}(\bar{\rho} \tilde{\mathbf{u}}) + \nabla \cdot \left(\bar{\rho} \tilde{\mathbf{u}} \otimes \tilde{\mathbf{u}} + \frac{\bar{p}}{M^2} \mathbf{I} \right) = \nabla \cdot \bar{\boldsymbol{\tau}} - \nabla \cdot \mathbf{T}, \quad (2)$$

where

$$\bar{\boldsymbol{\tau}} = \overline{\frac{\mu}{Re} \left[-\frac{2}{3}(\nabla \cdot \mathbf{u})\mathbf{I} + (\nabla \mathbf{u} + \nabla \mathbf{u}^T) \right]}.$$

- Filtered Species:

$$\frac{\partial}{\partial t}(\bar{\rho} \tilde{Y}_i) + \nabla \cdot (\bar{\rho} \tilde{Y}_i \tilde{\mathbf{u}}) = \nabla \cdot \bar{\mathbf{q}}_i - \nabla \cdot \bar{\mathbf{S}}_i + \bar{\dot{\omega}}_i \quad i = 1, \dots, N - 1, \quad (3)$$

where

$$\bar{\mathbf{q}}_i = \overline{\frac{\mu}{Sc_i Re} \nabla Y_i}.$$

Many additional terms arise as consequence of filtering compressible multicomponent conservation equations

- Filtered Total Energy:

$$\begin{aligned} \frac{\partial}{\partial t}(\bar{\rho}\tilde{e}_t) + \nabla \cdot [(\bar{\rho}\tilde{e}_t + \bar{p})\tilde{\mathbf{u}}] &= \nabla \cdot (\bar{\mathbf{q}}_e + M^2(\bar{\boldsymbol{\tau}} \cdot \tilde{\mathbf{u}})) \\ &- \nabla \cdot (\mathbf{Q} + M^2(\mathbf{T} \cdot \tilde{\mathbf{u}})) \\ &- \nabla \cdot \left[\frac{M^2}{2} \text{tr}(\mathbf{T}\tilde{\mathbf{u}}'') \right] + \nabla \cdot (M^2(\overline{\boldsymbol{\tau} \cdot \mathbf{u}}'')) + \bar{\dot{Q}}_e, \end{aligned} \quad (4)$$

where

$$\begin{aligned} \tilde{e}_t &= \tilde{e} + \frac{M^2}{2} \tilde{\mathbf{u}} \cdot \tilde{\mathbf{u}} + \frac{M^2}{2} \frac{\text{tr}(\mathbf{T})}{\bar{\rho}}, \\ \tilde{e} &= \sum_{i=1}^N \tilde{h}_i \tilde{Y}_i - \frac{\bar{p}}{\bar{\rho}} + \sum_{i=1}^N \left[(\widetilde{\tilde{h}_i \tilde{Y}_i} - \tilde{h}_i \tilde{Y}_i) + (\widetilde{\tilde{h}_i Y_i''} + \widetilde{h_i'' \tilde{Y}_i}) + \widetilde{h_i'' Y_i''} \right], \\ \bar{\dot{Q}}_e &= - \sum_{i=1}^N \bar{\dot{\omega}}_i h_{f_i}^\circ, \text{ and } \bar{\mathbf{q}}_e = \overline{\frac{\mu C_p}{Pr Re} \nabla T} + \sum_{i=1}^N \overline{h_i \mathbf{q}_i}. \end{aligned}$$

Many additional terms arise as consequence of filtering compressible multicomponent conservation equations

- Filtered Total Energy:

$$\begin{aligned}
 \frac{\partial}{\partial t}(\bar{\rho}\tilde{e}_t) + \nabla \cdot [(\bar{\rho}\tilde{e}_t + \bar{p})\tilde{\mathbf{u}}] &= \nabla \cdot (\bar{\mathbf{q}}_e + M^2(\bar{\boldsymbol{\tau}} \cdot \tilde{\mathbf{u}})) \\
 &\quad - \nabla \cdot (\mathbf{Q} \rightarrow M^2(\mathbf{T} \cdot \tilde{\mathbf{u}})) \\
 &\quad - \nabla \cdot \left[\frac{M^2}{2} \text{tr}(\mathbf{T}\tilde{\mathbf{u}}'') \right] + \nabla \cdot (M^2(\overline{\boldsymbol{\tau} \cdot \mathbf{u}}'')) + \bar{\dot{Q}}_e,
 \end{aligned} \tag{4}$$

- Transport due to the production of turbulent kinetic energy and work done under the action of the subfilter turbulence field

- Transport of turbulent kinetic energy due to the presence of subfilter turbulent fluctuations

Second and third terms typically neglected

- Transport due to
 - dissipation of filtered internal energy due to subfilter interactions
 - diffusive transport of turbulent kinetic energy
 - dissipation of subfilter turbulent kinetic energy
 - work due to mean shear stress interactions with the subfilter turbulence field

Consistent modeling of SFS covariances rare, enthalpy/EOS must also be filtered and require closures

- Turbulent Momentum, Energy, and Species Fluxes:

$$\mathbf{T} = \bar{\rho}(\widetilde{\tilde{\mathbf{u}} \otimes \tilde{\mathbf{u}}} - \tilde{\mathbf{u}} \otimes \tilde{\mathbf{u}}) + \bar{\rho}(\widetilde{\tilde{\mathbf{u}} \otimes \mathbf{u}''} + \widetilde{\mathbf{u}'' \otimes \tilde{\mathbf{u}}}) + \bar{\rho}\widetilde{\mathbf{u}'' \otimes \mathbf{u}''}$$

$$\mathbf{Q} = \bar{\rho}(\widetilde{\tilde{h}\tilde{\mathbf{u}}} - \tilde{h}\tilde{\mathbf{u}}) + \bar{\rho}(\widetilde{\tilde{h}\mathbf{u}''} + \widetilde{h''\tilde{\mathbf{u}}}) + \bar{\rho}\widetilde{h''\mathbf{u}''}$$

$$\mathbf{S}_i = \bar{\rho}(\widetilde{\tilde{Y}_i\tilde{\mathbf{u}}} - \tilde{Y}_i\tilde{\mathbf{u}}) + \bar{\rho}(\widetilde{\tilde{Y}_i\mathbf{u}''} + \widetilde{Y_i''\tilde{\mathbf{u}}}) + \bar{\rho}\widetilde{Y_i''\mathbf{u}''}$$

- Enthalpy:

$$\bar{\rho}\tilde{e} + \bar{p} = \bar{\rho} \sum_{i=1}^N \tilde{h}_i \tilde{Y}_i + \bar{\rho} \sum_{i=1}^N \left[(\widetilde{\tilde{h}_i \tilde{Y}_i} - \tilde{h}_i \tilde{Y}_i) + (\widetilde{\tilde{h}_i Y_i''} + \widetilde{h_i'' \tilde{Y}_i}) + \widetilde{h_i'' Y_i''} \right]$$

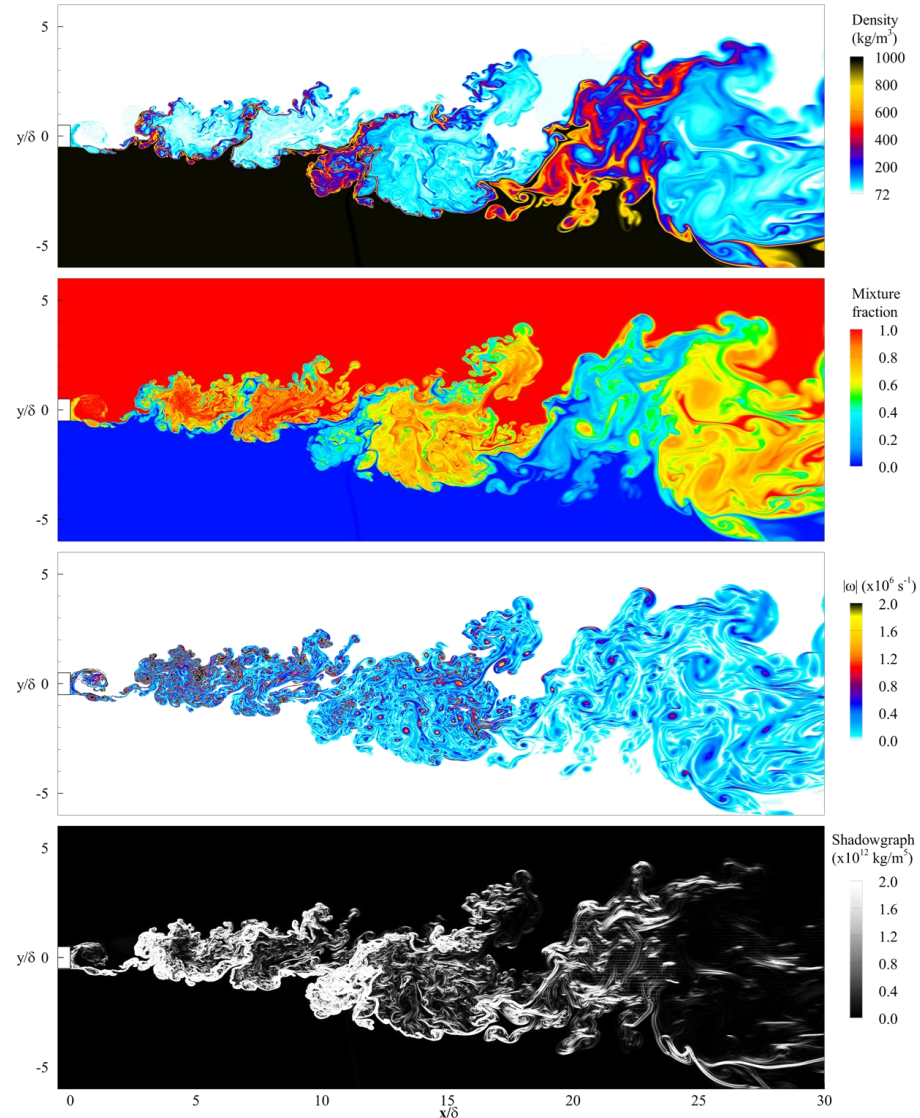
- Equation of State:

$$\bar{p} = \bar{\rho} R_u \sum_{i=1}^N \left(\frac{\tilde{T} \tilde{Y}_i}{W_i} + \frac{(\widetilde{\tilde{T} \tilde{Y}_i} - \tilde{T} \tilde{Y}_i) + (\widetilde{\tilde{T} Y_i''} + \widetilde{T'' \tilde{Y}_i}) + \widetilde{T'' Y_i''}}{W_i} \right)$$

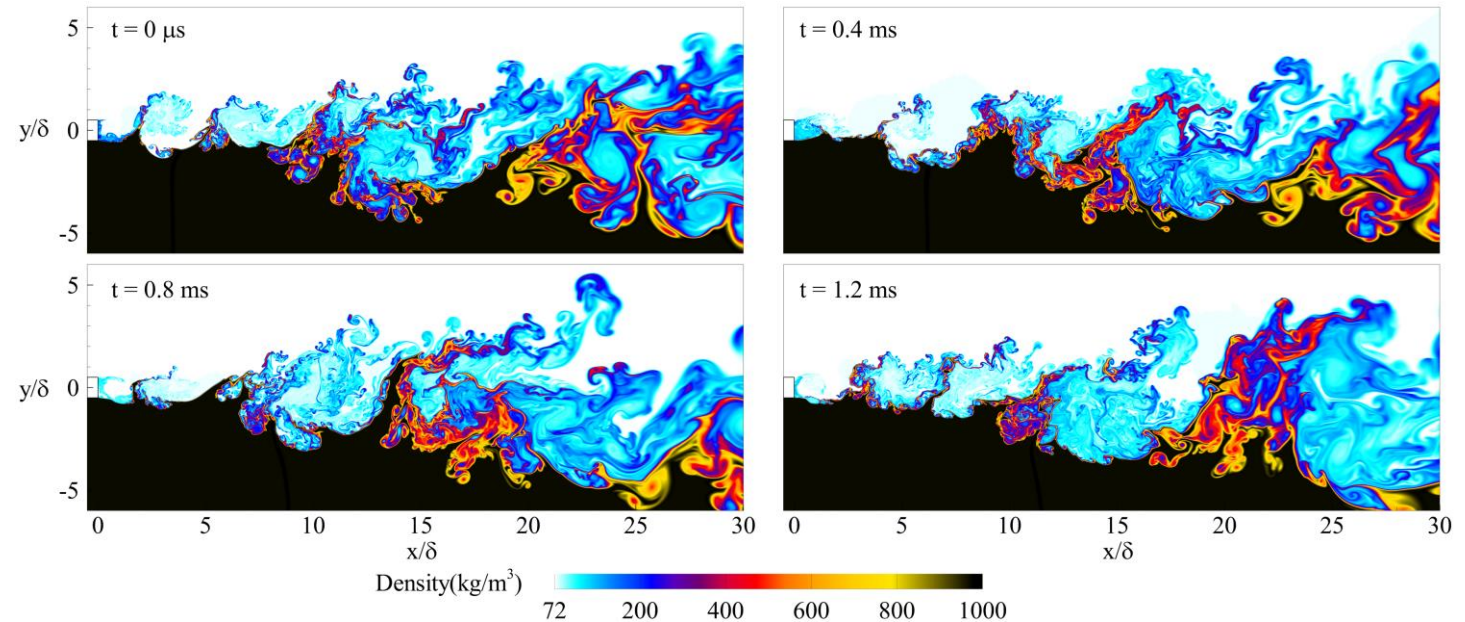
- Filtered Viscous Stress Tensor, and Filtered Energy and Mass Diffusion Fluxes

Analysis of mixing and turbulence-chemistry interactions via nonreacting and reacting $\text{CH}_4\text{-O}_2$ mixing layers

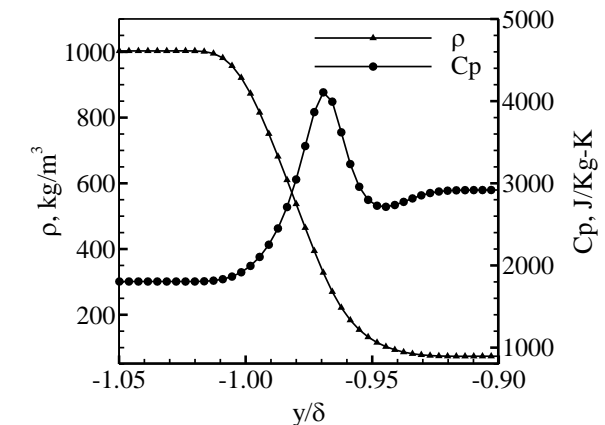
Instantaneous fields



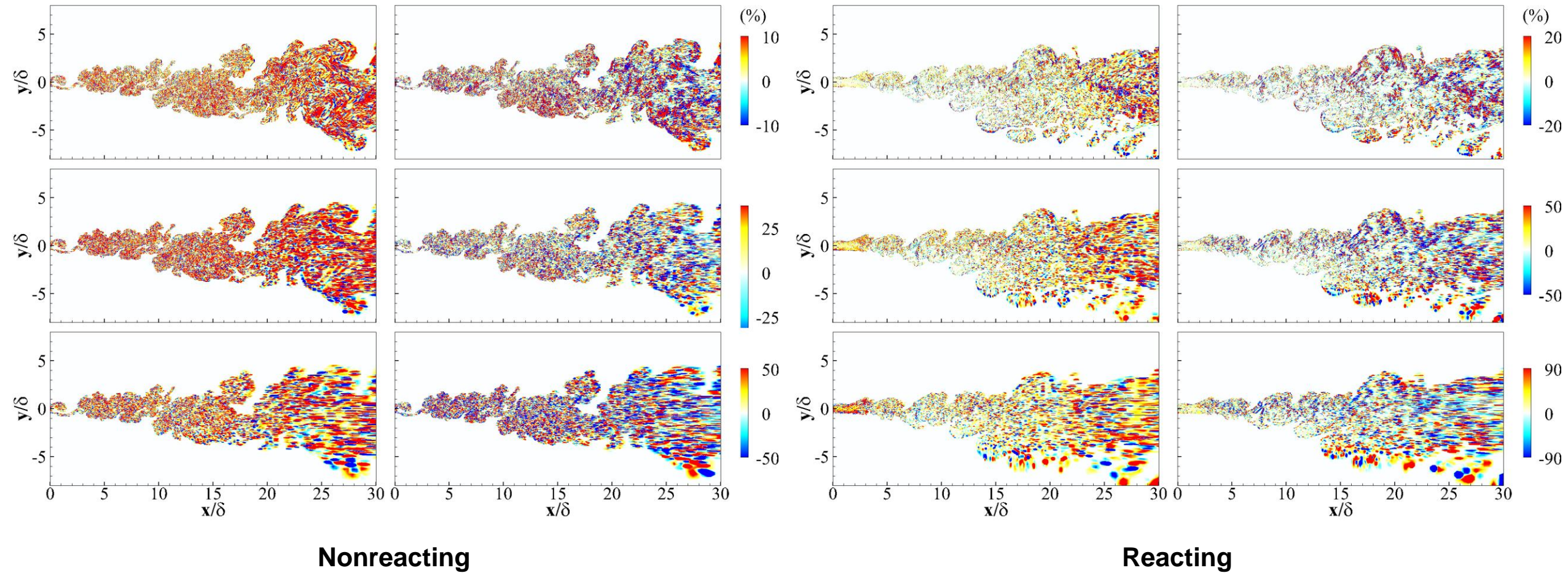
Temporal evolution of density field



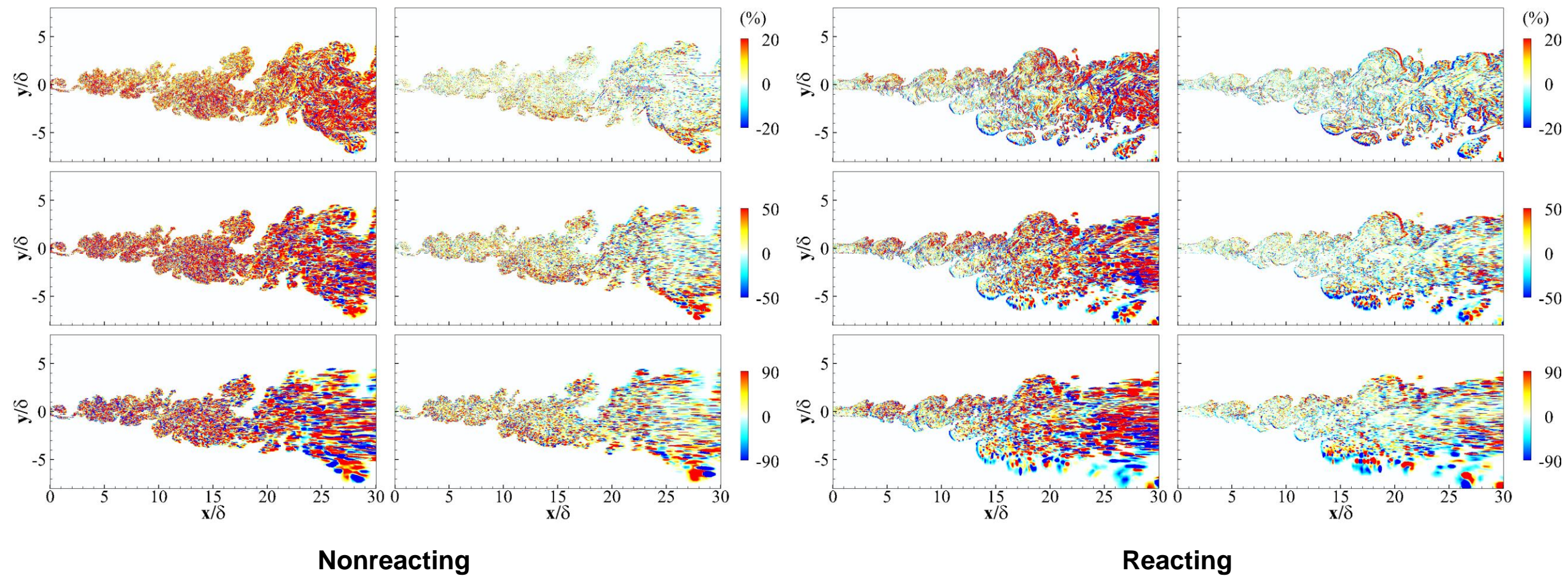
Transverse variation in density and specific heat



Relative magnitude of subfilter viscous flux terms with cutoffs of 2x, 5x, 10x Kolmogorov scale



Relative magnitude of subfilter diffusive heat flux terms with cutoffs of 2x, 5x, 10x Kolmogorov scale



Benefits of explicitly filtered LES to minimize these errors currently being investigated

Consistent modeling of SFS covariances rare, enthalpy/EOS must also be filtered and require closures

- Turbulent Momentum, Energy, and Species Fluxes:

$$\mathbf{T} = \bar{\rho}(\widetilde{\tilde{\mathbf{u}} \otimes \tilde{\mathbf{u}}} - \tilde{\mathbf{u}} \otimes \tilde{\mathbf{u}}) + \bar{\rho}(\widetilde{\tilde{\mathbf{u}} \otimes \mathbf{u}''} + \widetilde{\mathbf{u}'' \otimes \tilde{\mathbf{u}}}) + \bar{\rho}\widetilde{\mathbf{u}'' \otimes \mathbf{u}''}$$

$$\mathbf{Q} = \bar{\rho}(\widetilde{\tilde{h}\tilde{\mathbf{u}}} - \tilde{h}\tilde{\mathbf{u}}) + \bar{\rho}(\widetilde{\tilde{h}\mathbf{u}''} + \widetilde{h''\tilde{\mathbf{u}}}) + \bar{\rho}\widetilde{h''\mathbf{u}''}$$

$$\mathbf{S}_i = \bar{\rho}(\widetilde{\tilde{Y}_i\tilde{\mathbf{u}}} - \tilde{Y}_i\tilde{\mathbf{u}}) + \bar{\rho}(\widetilde{\tilde{Y}_i\mathbf{u}''} + \widetilde{Y_i''\tilde{\mathbf{u}}}) + \bar{\rho}\widetilde{Y_i''\mathbf{u}''}$$

- Enthalpy:

$$\bar{\rho}\tilde{e} + \bar{p} = \bar{\rho} \sum_{i=1}^N \tilde{h}_i \tilde{Y}_i + \bar{\rho} \sum_{i=1}^N \left[(\widetilde{\tilde{h}_i \tilde{Y}_i} - \tilde{h}_i \tilde{Y}_i) + (\widetilde{\tilde{h}_i Y_i''} + \widetilde{h_i'' \tilde{Y}_i}) + \widetilde{h_i'' Y_i''} \right]$$

- Equation of State:

$$\bar{p} = \bar{\rho} R_u \sum_{i=1}^N \left(\frac{\tilde{T} \tilde{Y}_i}{W_i} + \frac{(\widetilde{\tilde{T} \tilde{Y}_i} - \tilde{T} \tilde{Y}_i) + (\widetilde{\tilde{T} Y_i''} + \widetilde{T'' \tilde{Y}_i}) + \widetilde{T'' Y_i''}}{W_i} \right)$$

- Filtered Viscous Stress Tensor, and Filtered Energy and Mass Diffusion Fluxes

“Mixed” Dynamic Smagorinsky (DMM) model shown below is consistent, DSM is not since it neglects terms

- Eddy Viscosity:

$$\mu_t = \bar{\rho} C_R \Delta^2 \Pi_{\tilde{\mathbf{S}}}^{\frac{1}{2}} \quad \Pi_{\tilde{\mathbf{S}}} = \tilde{\mathbf{S}} : \tilde{\mathbf{S}} \quad \tilde{\mathbf{S}} = \frac{1}{2} (\nabla \tilde{\mathbf{u}} + \nabla \tilde{\mathbf{u}}^T)$$

- Stress Tensor:

$$\vec{\mathcal{T}} = (\vec{\tau} - \mathbf{T}) = (\mu_t + \mu) \frac{1}{Re} \left[-\frac{2}{3} (\nabla \cdot \tilde{\mathbf{u}}) \mathbf{I} + (\nabla \tilde{\mathbf{u}} + \nabla \tilde{\mathbf{u}}^T) \right] - \bar{\rho} \left(\widetilde{\tilde{\mathbf{u}} \otimes \tilde{\mathbf{u}}} - \tilde{\mathbf{u}} \otimes \tilde{\mathbf{u}} \right) - \frac{1}{3} \bar{\rho} q_{\text{sfs}}^2 \mathbf{I}$$

- Energy Flux:

$$\vec{\mathcal{Q}}_e = (\bar{\mathbf{q}}_e - \mathbf{Q}) = \left(\frac{\mu_t}{Pr_t} + \frac{\mu}{Pr} \right) \frac{1}{Re} \nabla \tilde{h} + \sum_{i=1}^N \tilde{h}_i \vec{\mathcal{S}}_i - \bar{\rho} \left(\widetilde{\tilde{h} \tilde{\mathbf{u}}} - \tilde{h} \tilde{\mathbf{u}} \right)$$

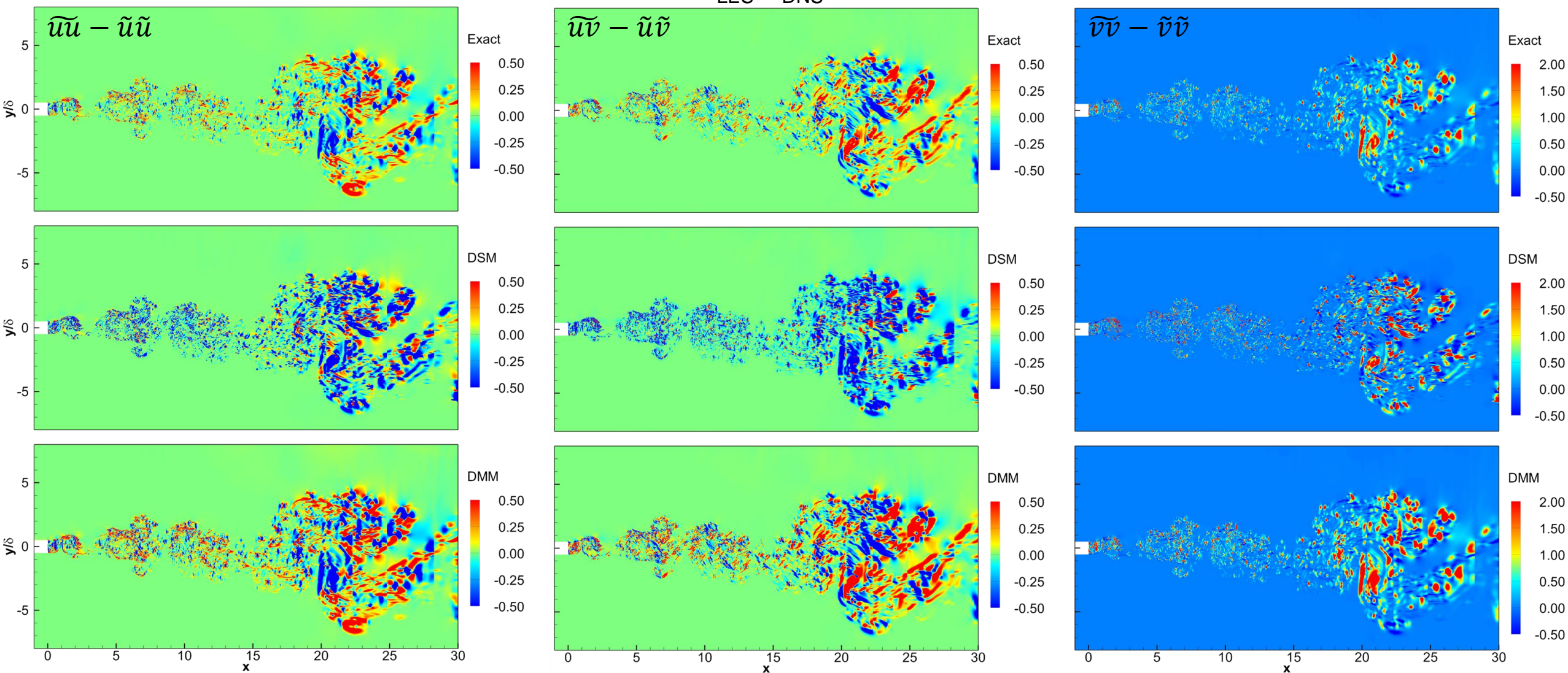
- Mass Flux:

$$\vec{\mathcal{S}}_i = (\bar{\mathbf{q}}_i - \mathbf{S}_i) = \left(\frac{\mu_t}{Sc_{t_i}} + \frac{\mu}{Sc_i} \right) \frac{1}{Re} \nabla \tilde{Y}_i - \bar{\rho} \left(\widetilde{\tilde{Y}_i \tilde{\mathbf{u}}} - \tilde{Y}_i \tilde{\mathbf{u}} \right)$$

Coefficients C_R , Pr_t , and Sc_{t_i} evaluated dynamically as functions of space and time

A priori assessment of Dynamic Smagorinsky (DSM) versus Mixed Dynamic Smagorinsky (DMM) models

$$\Delta_{\text{LES}}/\Delta_{\text{DNS}} = 5$$



***A priori* assessment of Dynamic Smagorinsky (DSM) versus Mixed Dynamic Smagorinsky (DMM) models**

Covariance	Dynamic Smagorinsky	Mixed Dynamic Smagorinsky
$(\widetilde{uu})_{\text{sfs}}$	65.7 %	82.8 %
$(\widetilde{uv})_{\text{sfs}}$	84.2 %	89.8 %
$(\widetilde{vv})_{\text{sfs}}$	53.0 %	90.7 %
$(\widetilde{uT})_{\text{sfs}}$	69.8 %	92.2 %
$(\widetilde{vT})_{\text{sfs}}$	74.8 %	91.0 %
$(\widetilde{uY})_{\text{sfs}}$	68.0 %	74.6 %
$(\widetilde{vY})_{\text{sfs}}$	61.6 %	92.7 %

Filter size 5x larger relative to DNS ($\Delta = 5$).

***A priori* assessment of Dynamic Smagorinsky (DSM) versus Mixed Dynamic Smagorinsky (DMM) models**

Covariance		Dynamic Smagorinsky	Mixed Dynamic Smagorinsky
$(\widetilde{uv})_{\text{sfs}}$	$\Delta = 5$	84.2 %	89.8 %
	$\Delta = 10$	17.2 %	60.9 %
$(\widetilde{uT})_{\text{sfs}}$	$\Delta = 5$	69.8 %	92.2 %
	$\Delta = 10$	9.3 %	33.5 %
$(\widetilde{vY})_{\text{sfs}}$	$\Delta = 5$	61.6 %	92.7 %
	$\Delta = 10$	18.8 %	58.9 %

Provides baseline data required to establish subfilter model resolution requirements which are by definition dependent on the system of models employed and the use of implicit versus explicit filtering, etc. Future work will focus on quantifying these requirements.

Subfilter modeling of the equation of state

- Errors arise from computing the filtered quantities directly from the resolved flow variables in EOS for multicomponent systems, i.e.

$$\bar{p} = \overline{Z\rho RT} = \bar{\rho}\widetilde{ZRT}$$

$$\bar{p} = \bar{\rho}\tilde{Z}\tilde{R}\tilde{T} + \bar{\rho}(\widetilde{ZRT} - \tilde{Z}\tilde{R}\tilde{T})$$

- The subfilter covariance term has historically been neglected
- Note that this can also be represented in terms of a residual density as follows

$$\overline{\rho_{exact}} = \frac{\bar{p}}{\widetilde{ZRT}}$$

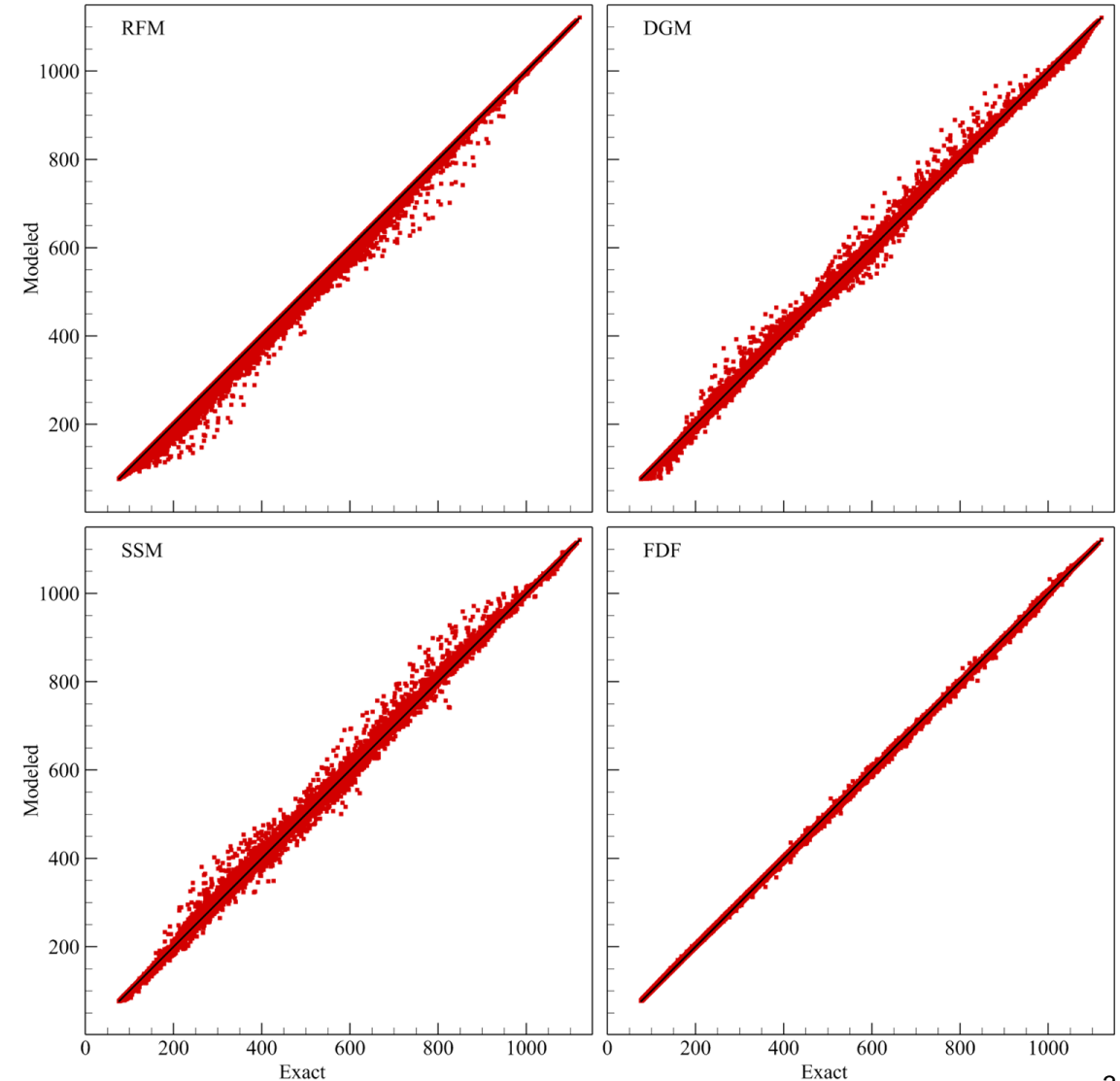
$$\overline{\rho_{LES}} = \frac{\bar{p}}{\tilde{Z}\tilde{R}\tilde{T}}$$

$$\rho_{sfs} = \overline{\rho_{LES}} - \overline{\rho_{exact}} = \frac{\bar{p}}{\tilde{Z}\tilde{R}\tilde{T}} - \frac{\bar{p}}{\widetilde{ZRT}}$$

Four approaches have been considered to model the EOS subfilter covariance field

Model	Correlation Coefficient		L^2 -error	
	$\Delta_f = 5$	10	5	10
No-model			11.3	76.15
Reynolds-filtered	-0.94	-0.95	6.76	52.82
Dynamic Gradient	0.78	0.70	4.43	37.39
Scale-similarity	0.75	0.63	4.75	43.39
Presumed FDF	0.97	0.97	1.64	6.44

Filtered density via DNS compared to LES [kg/m³]

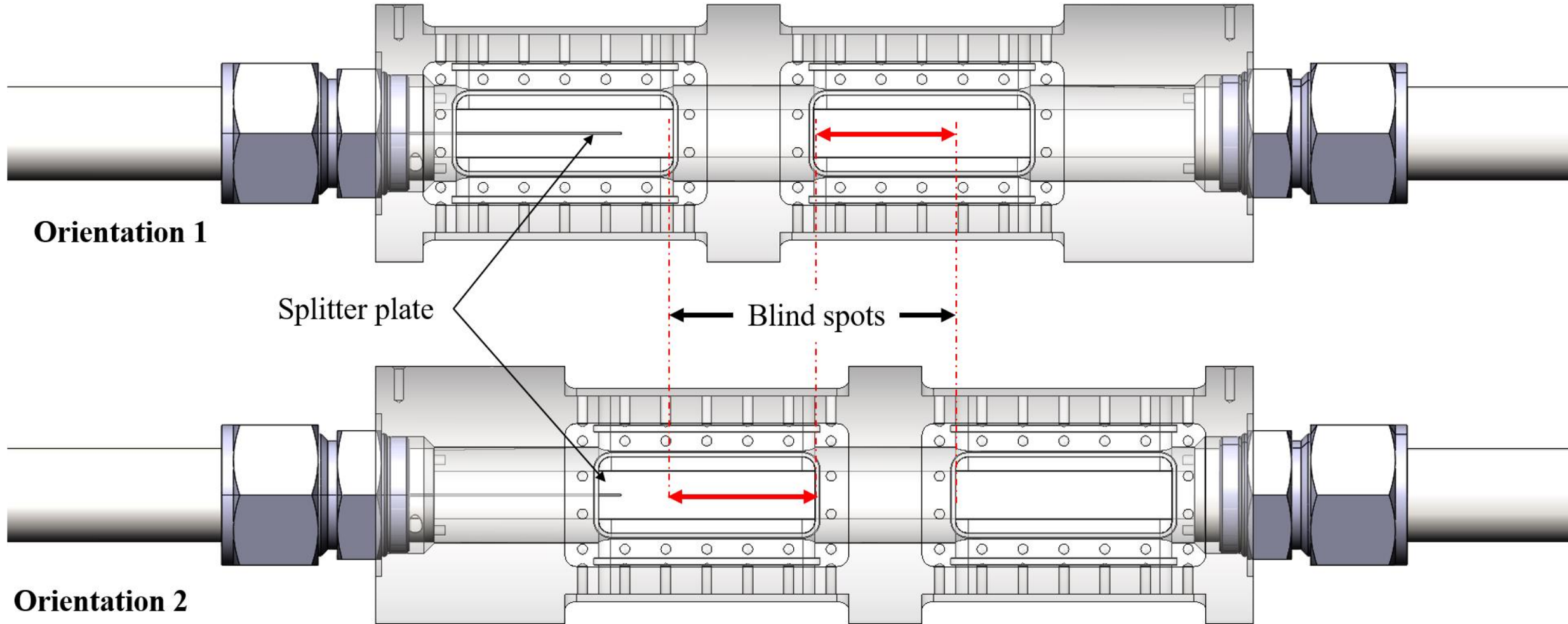


Summary

- Investigations have provided new insights and workflow required to perform $O(1\text{-billion})$ cell 3D DNS and successive LES with emphasis on establishing refined precision and control of errors
- Have addressed challenges related to LES subfilter modeling for compressible flows
 - Treatment of additional terms that appear in the filtered compressible conservation equations
 - Model consistency, optimization, and development of quantified resolution requirements
 - Future work ... investigate needs related to subfilter scalar-scalar covariance fields and the filtered mass, momentum, energy diffusion fluxes (e.g., model plus required resolution)
- Investigated anomalies associated with multiscale mixing and combustion
 - Thermodynamic nonidealities and transport anomalies impose additional nonlinearities that modulate broadband turbulence characteristics and observables (e.g., compressibility effects)
 - Future work ... investigate needs related to filtered EOS, thermodynamic, and transport properties (e.g., modeling nonequilibrium turbulence, baroclinic torque, Favre-versus Reynolds-averaging)
- Findings facilitate more precise application of LES guided by quantified implementation requirements and refined control of errors associated with filtering

Thank You!

Test section is designed to give full optical access across the entire axial span of the mixing layer

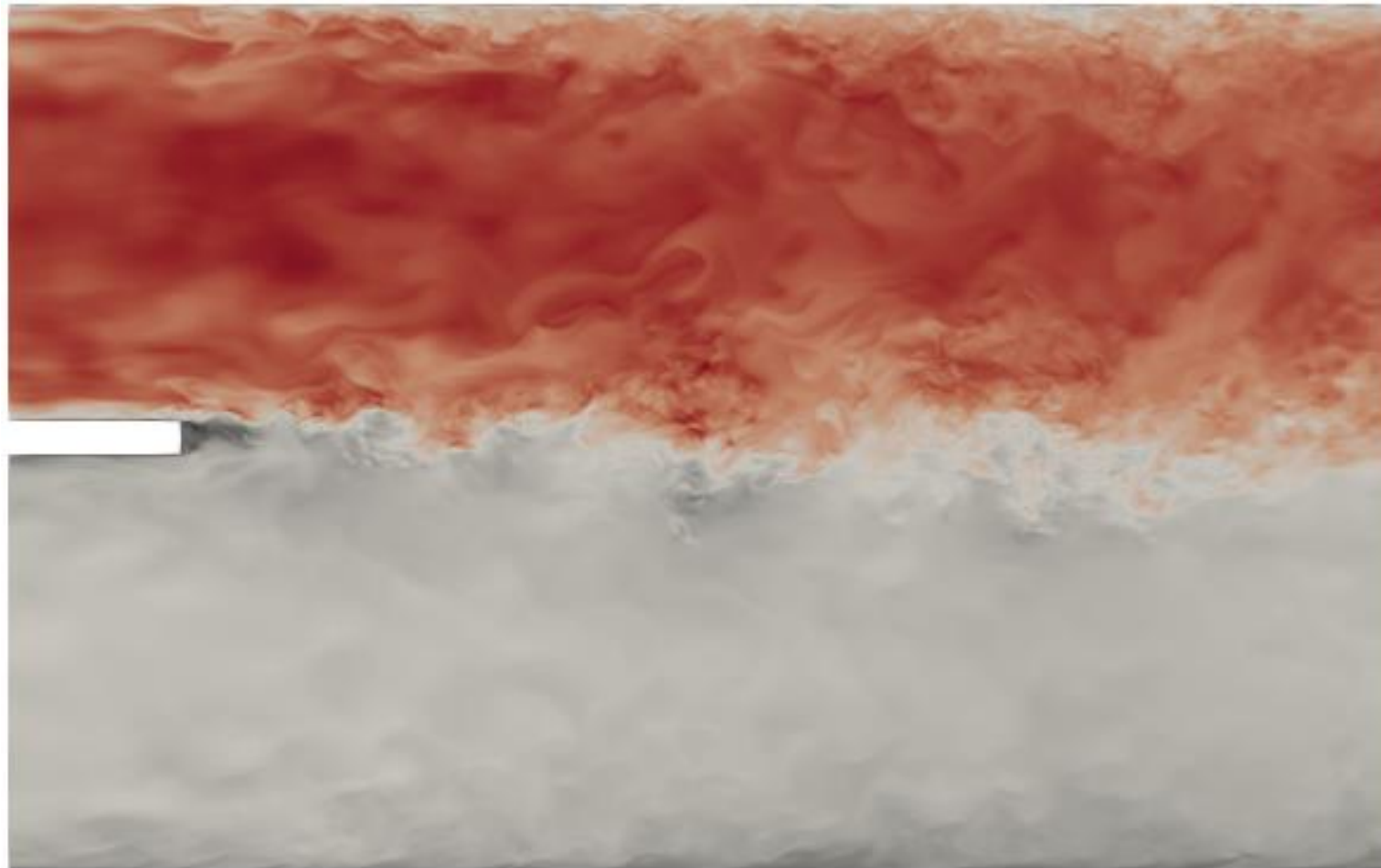


Experimental conditions and techniques

	Pressure	Temperature(C)		Velocity (m/s)		Velocity Ratio (r)	Density Ratio (s)	Atwood Number	Reynolds Number	Technique
Baseline	1160	45	35	0.53	0.11	0.21	1.73	0.27	9e4 – 1e5	Shadowgraphy, Raman Scattering
Flipped V	1160	45	35	0.17	0.37	2.22	1.73	0.27		Shadowgraphy, Raman Scattering
Flipped T,V	1160	35	45	0.19	0.51	2.77	0.58	0.27		Shadowgraphy
High baseline and flipped cases	1160	45	40	0.59	0.33	0.57	1.15	0.07		Schlieren
	1160	45	40	0.68	0.51	0.75	1.15	0.07		Schlieren
	1160	45	40	0.32	0.46	1.45	1.15	0.07		Schlieren
	1160	40	45	0.46	0.30	0.65	0.87	0.07		Schlieren
	1160	40	45	0.54	0.49	0.91	0.87	0.07		Schlieren
	1160	40	45	0.32	0.42	1.31	0.87	0.07		Schlieren

- High-speed Shadowgraphy
- High-speed Schlieren
- Spontaneous Raman Scattering

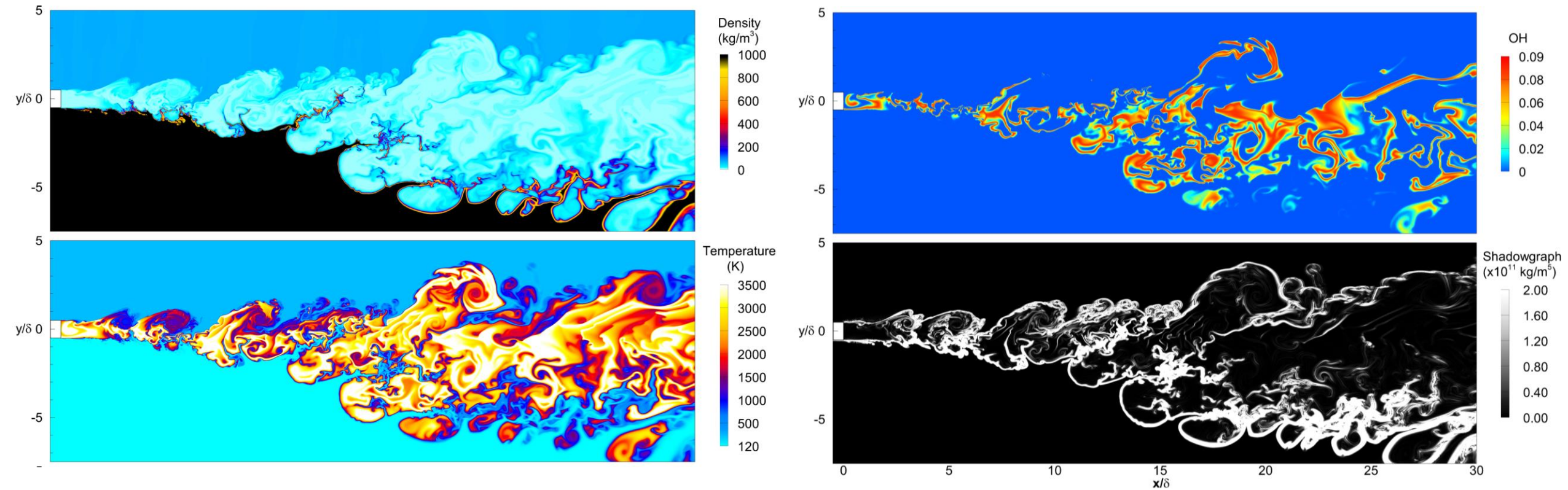
Cross-section of instantaneous axial velocity



Non-Dimensional U-Velocity



Analysis of mixing and turbulence-chemistry interactions via nonreacting $\text{CH}_4\text{-O}_2$ mixing layers



Representative instantaneous fields